Monsoons Climate Change Assessment

Bin Wang[1], Michela Biasutti[2], Michael P. Byrne[3,4], Christopher Castro[4], Chih-Pei Chang[5,6], Kerry Cook[7], Rong Fu[8], Alice M. Grimm[9], Kyung-Ja Ha[10,11,12], Harry Hendon[13], Akio Kitoh[14,15], R. Krishnan[16], June-Yi Lee[11,12], Jianping Li[17], Jian Liu[18], Aurel Moise[19], Salvatore Pascale[20], M. K. Roxy[16], Anji Seth[21], Chung-Hsiung Sui[6], Andrew Turner[22,23], Song Yang[24,25], Kyung-Sook Yun[11], Lixia Zhang[26], Tianjun Zhou[26]

[1] Department of Atmospheric Sciences, University of Hawaii, Honolulu, HI, USA

[2] Lamont-Doherty Earth Observatory, Columbia University, Palisades, NY, USA

[3] School of Earth & Environmental Sciences, University of St Andrews, St. Andrews, UK

[4] Department of Physics, University of Oxford, Oxford, UK

[4] Department of Hydrology and Atmospheric Sciences, University of Arizona, Tucson, AZ, USA

[5] Department of Meteorology, Naval Postgraduate School, Monterey, CA, USA

[6] Department of Atmospheric Sciences, National Taiwan University, Taipei, Taiwan

[7] Department of Geological Sciences, University of Texas, Austin, TX, USA

[8] Department of Atmospheric and Oceanic Sciences, University of California, Los Angeles, CA, USA

[9] Department of Physics, Federal University of Paraná, Curitiba, Brazil

[10] Department of Atmospheric Sciences, Pusan National University, Busan, Republic of Korea

[11] Institute for Basic Science, Center for Climate Physics, Busan, Republic of Korea

[12] Research Center for Climate Sciences and Department of Climate System, Pusan National

University, Busan, Republic of Korea

[13] Bureau of Meteorology, Melbourne, Australia

[14] Japan Meteorological Business Support Center, Tsukuba, Japan

[15] Meteorological Research Institute, Tsukuba, Japan

[16] Indian Institute of Tropical Meteorology, Pune, India

[17] Ocean University of China, Qingdao, China

[18] Nanjing Normal University, Nanjing, China

[19] Center for Climate Research Singapore, Republic of Singapore

[20] Department of Earth System Sciences, Stanford University, Stanford, CA, USA

[21] Department of Geography, University of Connecticut, Storrs, CT, USA

[22] Department of Meteorology, University of Reading, Reading, UK

[23] National Centre for Atmospheric Science, University of Reading, Reading, UK

[24] School of Atmospheric Sciences and Guangdong Province Key Laboratory for Climate Change and Natural Disaster Studies, Sun Yat-sen University, Guangzhou, China

[25] Southern Marine Science and Engineering Guangdong Laboratory (Zhuhai), China

[26] Institute of Atmospheric Physics, Chineses Academy of Sciences, China

Corresponding Author: Dr. Chih-Pei Chang, email:cpchang@nps.edu

Abstract

Monsoon rainfall has profound economic and societal impacts for more than two-thirds of the global population. Here we provide a concise review on past monsoon changes and their primary drivers, the projected future changes and key physical processes, and discuss challenges of the present and future modeling and outlooks. Continued global warming and urbanization over the past century has already caused a significant rise in the intensity and frequency of extreme rainfall events in all monsoon regions (high confidence). Observed changes in the mean monsoon rainfall vary by region with significant decadal variations. NH land monsoon rainfall as a whole declined from 1950 to 1980 and rebounded after the 1980s, due to the competing influences of internal climate variability and radiative forcing from GHGs and aerosol forcing (high confidence); however, it remains a challenge to quantify their relative contributions.

The CMIP6 models improve upon the simulation of global monsoon intensity and precipitation climatology compared to CMIP5 models, but common model biases and large intermodal spreads in projections persist. Nevertheless, there is high confidence that the frequency and intensity of monsoon extreme rainfall events will increase, alongside an increasing risk of drought over some monsoon regions. Also, there is high confidence that land monsoon rainfall will increase in South Asia and East Asia, and medium confidence that it will increase in northern Africa and decrease in North America, but remain unchanged in Southern Hemisphere monsoon regions. Over the Asian-Australian monsoon region the variability of monsoon rainfall is projected to increase on daily to decadal time scales. In spite of considerable variations between different regions, the rainy season will likely be lengthened in the Northern Hemisphere due to late retreat (especially over East Asia), but shortened in the Southern Hemisphere due to delayed onset.

Capsule Summary

This paper reviews the current knowledge on detection, attribution and projection of global and regional monsoons (South Asian, East Asian, Australian, South American, North American, and African) under climate change.

1. Introduction

Many parts of the Earth's surface and two-thirds of the global population are influenced by the monsoon. This paper reviews the current state of knowledge of climate change and its impacts on the global monsoon and its regional components, including recent results from phase six of the Coupled Model Intercomparison Project (CMIP6) that were reported at a World Meteorological Organization/World Weather Research Programme workshop held in Zhuhai in early December 2019. The review's primary focus is on monsoon rainfall, both mean and extremes, whose variability has tremendous economic and societal impacts. Due to the large body of literature on this broad topic, only a fraction can be cited in this concise review.

The global monsoon (GM) is a defining feature of the Earth's climate and a forced response of the coupled climate system to the annual cycle of solar insolation. For clarity, we define the monsoon domain primarily based on rainfall contrast in the solstice seasons (Fig. 1). The North American monsoon (NAM) domain covers western Mexico and Arizona, but also Central America and Venezuela, and is larger than that traditionally recognized by many scientists working on the NAM. We aim to encompass the range of literature marrying together global monsoon, regional monsoon and paleoclimate monsoon perspectives and therefore reach a compromise. Equatorial Africa and the Maritime Continent also feature annual reversal of surface winds, although the former has a double peak in the equinoctial seasons and the latter is heavily influenced by complex terrain (Chang 2004).

Our goal is to outline past changes of the monsoon and identify the key drivers of these changes, assess the roles and impacts of natural and anthropogenic forcings and regional variability, and discuss the limitations and difficulties of current climate models in representing

monsoon variability. We will also attempt to summarize projected future changes both globally and in various monsoon regions using recent model results. Due to the inherent uncertainties and model limitations, the degree of confidence in the results varies. A section on model issues and outlook is devoted to discussing challenges of present and future monsoon modeling.

2. Global monsoon

2.1. Detection and Attribution of observed changes

Wang and Ding (2006) found a decreasing trend of global land monsoon precipitation from the 1950s to 1980, mainly due to the declining monsoon in the northern hemisphere (NH). After 1980, GM precipitation (GMP) has intensified due to a significant upward trend in the NH summer monsoon (Wang et al., 2012). Extended analysis of the whole 20th century NH land monsoon rainfall indicates that short-period trends may be part of multidecadal variability, which is primarily driven by forcing from the Atlantic (Atlantic Multidecadal Variation; AMV, and the Pacific (Interdecadal Pacific Oscillation; IPO) (Zhou et al. 2008, Wang et al. 2013, 2018; Huang et al. 2020a). On the other hand, there is evidence that anthropogenic aerosols have influenced decreases of NH land monsoon precipitation in the Sahel, South and East Asia during the second half of the 20th century (Polson et al., 2014; Giannini and Kaplan, 2019; Zhou et al., 2020b). It should be noted that this long-term decrease in precipitation could be, in part, due to natural multi-decadal variations of the regional monsoon precipitation (Sontakke et al. 2008, Jin and Wang 2017; Huang et al., 2020b). It remains a major challenge, however, to quantify the relative contributions of internal modes of variability versus anthropogenic forcing on the global scale.

2.2. Projected long-term changes

The CMIP5 results suggest that GM area, annual range and mean precipitation are likely to increase by the end of the 21st century (Kitoh et al., 2013; Hsu et al., 2013; Christensen et al., 2013). The increase will be stronger in the NH, and the NH rainy season is likely to lengthen due to earlier or unchanged onset dates and a delayed retreat (Lee and Wang, 2014). The increase in GM precipitation was primarily attributed to temperature-driven increases in specific humidity, resulting in the "wet-get-wetter" pattern (Held and Soden, 2006).

Analysis of 34 CMIP6 models indicates a larger increase in monsoon rainfall over land than over ocean in all four core Shared Socio-economic Pathways (SSPs) (Fig. 2; Lee et al. 2019). The projected GMP increase over land by the end of the 21st century relative to 1995-2014 in CMIP6 is about 50% larger than in CMIP5. Models with high (>4.2°C) equilibrium climate sensitivity (ECS) account for this larger projection. The causes of CMIP6 models' high ECS has been discussed in Zelinka et al. (2020). Note that the forced signal of GMP over land shows a decreasing trend from 1950 to the 1980s, but the trend reversed around 1990, which is consistent with the CMIP5 results (Lee and Wang, 2014). During 1950-1990, the temperature-driven intensification of precipitation was likely masked by a fast precipitation response to anthropogenic sulfate and volcanic forcing, even though the warming trend due to GHG since the pre-industrial period (1850-1900) is three times larger than the cooling due to aerosol forcing (Lau and Kim, 2017; Richardson et al. 2018;). The recent upward trend may signify the emergence of the greenhouse-gas signal against the rainfall reduction due to aerosol emissions. However, the trend during recent decades can be influenced by the leading modes of multidecadal variability of global SST (Wang et al. 2018). Lee et al. (2019) found that land monsoon precipitation sensitivity (precipitation change per degree of global warming) slightly increases with the level of GHG

forcing, whereas the ocean monsoon precipitation has almost no sensitivity (Fig. 2). The GM land precipitation sensitivity has a median of 0.8 %/°C in SSP2-4.5, and a median of 1.4%/°C in SSP5-8.5. The latter is slightly higher than that simulated by CMIP5 models under RCP 8.5.

Wang et al. (2020) examined the ensemble-mean projection from 15 early-released CMIP6 models, which estimates that under SSP2-4.5 the total NH land monsoon precipitation will increase by about 2.8%/°C in contrast to little change in the southern hemisphere (SH; -0.3%/°C). In both hemispheres, the annual range of land monsoon rainfall will increase by about 2.6%/°C, with wetter summers and drier winters. In addition, the projected land monsoon rainy season will be lengthened in the NH (by about ten days) due to late retreat, but will be shortened in the SH due to delayed onset; the interannual variations of GMP will be more strongly controlled by ENSO variability (Wang et al. 2020). In monsoon regions, increases in specific humidity are spatially uniform (Fig. 4b), but the rainfall change features a robust NH-SH asymmetry and an east-west asymmetry between enhanced Asian-African monsoons and weakened NAM (Fig. 4a), suggesting that circulation changes play a crucial role in shaping the spatial patterns and intensity of GM rainfall changes (Wang et al. 2020). GHG-induced horizontally differential heating results in a robust "NH-warmer-than-SH" pattern (Fig. 4c), which enhances NH monsoon rainfall (Liu et al. 2009, Mohtadi et al. 2016), especially in Asia and northern Africa, due to an enhanced thermal contrast between the large Eurasia-Africa landmass and adjacent oceans (Endo et al. 2018). Those CMIP models that project a stronger inter-hemispheric thermal contrast generate stronger Hadley circulations, more northward positions of the ITCZ, and enhanced NH monsoon precipitation (Wang et al. 2020). The GHG forcing also induces a warmer equatorial eastern Pacific (Fig. 4c), which reduces NAM rainfall by shifting the ITCZ equatorward (Wang et al. 2020).

Climate models on average predict weakening ascent under global warming (Endo and Kitoh, 2014), which tends to dry monsoon regions. Weakening monsoon ascent has been linked to the slowdown of the global overturning circulation (Held and Soden 2006). However, a definitive theory for why monsoon circulations broadly weaken with warming remains elusive.

Land monsoon rainfall (LMR) provides water resources for billions of people; an accurate prediction of its change is vital for the sustainable future of the planet. Regional land monsoon rainfall exhibits very different sensitivities to climate change (Fig. 3). The annual mean LMR in the East Asian and South Asian monsoons shows large positive sensitivities with means of 4.6%/°C, and 3.9%/°C, respectively, under SSP2-4.5. The LMR likely increases in NAF, but decreases in NAM, and remains unchanged in the Southern Hemisphere monsoons (Jin et al. 2020).

2.3. Projected near-term change

The interplay between internal modes of variability, such as IPO, AMV and SH Annular Mode (Zheng et al. 2014), and anthropogenic forcing is important in the historical record and for the near-term future (Chang et al. 2014). Huang et al. (2020a) used two sets of initial condition large ensembles to suggest that internal variability linked to the IPO could overcome the forced upward trend in the South Asian monsoon rainfall up to 2045. Using 20th-century observations and numerical experiments, Wang et al. (2018) showed that the hemispheric thermal contrast in the Atlantic and Indian Oceans and the IPO can be used to predict the NH land monsoon rainfall change a decade in advance. The significant decadal variability of monsoon rainfall leads to considerable uncertainties in climate projections for the next 30 years; thus, improvements in predicting internal modes of variability could reduce uncertainties in near-term climate projections.

3. Regional monsoon changes

3.1 South Asian monsoon

The South Asian summer monsoon (SASM) circulation experienced a significant declining trend from the 1950s together with a weakening local meridional circulation and notable precipitation decreases over north-central India and the west coast that are associated with a reduced meridional temperature gradient (e.g., Krishnan et al., 2013, Roxy et al. 2015). This trend was attributed to effects of anthropogenic aerosol forcing (e.g., Salzmann et al., 2014; Krishnan et al. 2016) and equatorial Indian Ocean warming due to increased GHG (e.g., Sabeerali and Ajayamohan 2017). However, it could potentially be altered by multidecadal variations (Shi et al. 2018) arising from internal modes of climate variability such as the IPO and AMV (e.g., Krishnan and Sugi, 2003, Salzmann and Cherian, 2015, Jiang and Zhou 2019). The processes by which aerosols affect monsoons were reviewed by Li et al. (2015). Aerosols can also have a remote impact on regional monsoons (Shaeki et al., 2018).

CMIP models consistently project increases in the mean and variability of SASM precipitation, despite weakened circulation at the end of the 21st century relative to the present (e.g., Kitoh et al. 2013; Wang et al. 2014), though some models disagree (Sabeerali and Ajayamohan 2017). The uncertainty in radiative forcing from aerosol emissions in CMIP5 causes a large spread in the response of SASM rainfall (Shonk et al., 2019). However, this is not the case in CMIP6 projections (Fig. 3).

3.2 East Asian monsoon

During the 20th century, East Asian summer monsoon (EASM) exhibited considerable multi-decadal variability with a weakened circulation and a south flood-north drought pattern

since the late 1970s (Zhou 2009; Ding et al. 2009). The south flood-north drought pattern has been predominantly attributed to internal variability, especially the phase change of the IPO (Li et al. 2010, Nigam et al 2015, Ha et al. 2020a), and aided by GHG-induced warming (Zhu et al. 2012), and increased Asian aerosols emissions from the 1970s to 2000s (Dong et al., 2019). Since 1979, both sea-surface temperature (SST) and atmospheric heating over Southeast Asia and adjacent seas have increased significantly (Li et al. 2016), which may have led to decreased rainfall over East Asia, South Asia (Annamalai et al., 2013) and the Sahel region (He et al. 2017).

Analysis of 16 CMIP6 models indicates that, under the SSP2-4.5 scenario, EASM precipitation will increase at 4.7 %/°C (Ha et al. 2020b), with dynamic effects more important than thermodynamic effects (Oh et al., 2018; Li et al. 2019). EASM duration is projected to lengthen by about five pentads due to earlier onset and delayed retreat (Ha et al. 2020b), which is comparable to previous assessment results (Endo et al. 2012, Kitoh et al. 2013, Moon and Ha 2017).

3.3 African monsoon

West Africa rainfall totals in the Sahel have been increasing since the 1980s, which helped regreening (Taylor et al. 2017; Brandt et al. 2019). Much of the increase in seasonal rainfall is owed to positive trends in mean intensity (Lodoun et al. 2013, Sarr et al. 2013), rainfall extremes (Panthou et al. 2014, Sanogo et al. 2015), and the frequency of intense mesoscale convective systems (Taylor et al. 2017). Several West African countries have experienced trends towards a wetter late season and delayed cessation of the rains (Lodoun et al. 2013, Brandt et al. 2019). All the above changes are qualitatively consistent with the CMIP5 response to GHG (Marvel et al., 2019). Preliminary results from CMIP6 confirm that the Sahel will become wetter, except for the

west coast, and the rainy season will extend later (Supplementary Fig. S1). Yet, the range of simulated variability has not improved, and large quantitative uncertainties in the projections persist. In spite of the large spread, the CMIP6 models project that NAF land monsoon rainfall will likely increase (Fig. 3).

In East Africa, observed increases in the boreal fall short rains are more robust (e.g., Cattani et al. 2018) than negative trends in the spring long rains (e.g., Maidment et al. 2015). Regionality is pronounced, and there is sensitivity to Indian Ocean SSTs and Pacific variability (Liebmann et al. 2014; Omondi et al. 2013). Selected CMIP6 models project little agreement on how East African rainfall will change (supplementary Fig. S2), while some regional models suggest enhanced rainfall during the short rains and a curtailed long-rains season (Cook and Vizy 2013; Han et al. 2019). In the Congo Basin, observed precipitation trends are inconclusive (Zhou et al. 2014; Cook and Vizy 2019), but one study reports earlier onset of the spring rains (Taylor et al. 2018). A preliminary analysis finds overall improvement in CMIP6 models in the overestimation of Congo Basin rainfall, though projections of changes under the SSP2-4.5 scenario are inconsistent. (Supplementary Fig. S3).

The CMIP6 models project that under SSP2-4.5 scenario and by the latter part of 21st century, the SAF land monsoon rainfall will likely increase in summer but considerably reduce in winter, so that the annual range will amplify but the annual mean rainfall will not change significantly (Fig. 3)

3.4 Australian monsoon

Observations show increasing trends in mean and extreme rainfall over northern, especially northwestern Australia since the early 1970s (Dey et al. 2019). Although Australian

summer monsoon rainfall has exhibited strong decadal variations during the 20th and early 21st century, making detection and attribution of trends challenging, the recent upward trend since 1970s has been attributed to direct thermal forcing by increasing SST in the tropical western Pacific (Li et al. 2013) and to aerosol and GHG forcing (Rotstayn et al. 2007, Salzmann 2016).

Australian monsoon rainfall is projected to increase by an average of 0.4%/°C in 33 CMIP5 models (Dey et al. 2019), although there is a large spread in the magnitude and even the direction of the projected change. By selecting the best performing models for the Australian monsoon, Joudain et al. (2013) found that seven of ten "good" CMIP5 models indicate a 5-20% increase in monsoon rainfall over northern (20°S) Australian land by the latter part of the 21st century, but trends over a much larger region of the Maritime Continent are more uncertain. Narsey et al. (2019) found that the range in Australian monsoon projections from the available CMIP6 ensemble is substantially reduced compared to CMIP5, however, models continue to disagree on the magnitude and direction of change. The CMIP6 models project that summer and annual mean LMR changes are insignificant under SSP2-4.5; but the winter LMR will likely decrease (Fig. 3) due to the enhanced Asian summer monsoon. By the end of the 21st century, the Madden-Julian Oscillation (MJO) is anticipated to have stronger amplitude rainfall variability (Maloney et al. 2018), but the impact on Australian summer monsoon intraseasonal variability is uncertain (Moise et al. 2019).

3.5 North American monsoon

Observed long-term 20th century rainfall trends are either negative or null, but the trends can vary substantially within this region (Pascale et al., 2019). During the period of 1950-2010 the monsoonal ridge was strengthened and shifted the patterns of transient inverted troughs

making them less frequent in triggering severe weather (Lahmers et al., 2016). Recent observational and modeling studies show an increase in the magnitude of extreme events in NAM and Central American rainfall under anthropogenic global warming (Aguilar et al., 2005; Luong et al., 2017).

Climate models suggest an early-to-late redistribution of the mean NAM precipitation with no overall reduction (Seth 2013, Cook and Seager, 2013), and a more substantial reduction for Central American precipitation (Colorado-Ruiz et al., 2019). However, there is low confidence in these projections, since both local biases (the models' representation of vegetation dynamics, land cover and use, soil moisture hydrology) and remote biases (current and future SST) may lead to large uncertainties (Bukovsky et al., 2015; Pascale et al., 2017). Confidence in mean precipitation changes is lower than in the projection that precipitation extremes are likely to increase due to the changing thermodynamic environment (Luong et al. 2017; Prein et al., 2016).

Figure 5 schematically sums up the factors that are likely to be determinant in the future behavior of the NAM: the expansion and northwestward shift of the NAM ridge, and the strengthening of the remote stabilizing effect due to SST warming are shown, and more intense MCS-type convection. More uncertain remains the future of the NAM moisture surges and the track of the upper-level inverted troughs, which are key synoptic processes controlling convective activity.

3.6 South American monsoon

A significant positive precipitation trend since the 1950s till the 1990s was observed in southeast South America, and has been related to interdecadal variability (Grimm and Saboia, 2015), ozone depletion and increasing GHG (Gonzalez et al. 2014; Vera and Diaz 2015). The trend

in the tropical South American monsoon is less coherent due to the influence of the tropical Atlantic and the tendency to reverse rainfall anomalies from spring to summer in the central-east South America due to land-atmosphere interactions (Grimm et al. 2007). In recent decades the dry season has been lengthened and become drier, especially over the southern Amazonia, which has significant influences on vegetation and moisture transport to the SAM core region (Fu et al. 2013).

The CMIP6 models-projected future precipitation changes resemble the anomalies expected for El Niño: little change of total precipitation (Figs. 3 and 4). This is consistent with El Niño impacts (Grimm 2011) and CMIP5 projections (Seth et al. 2013). CMIP5 also projected reduction of early monsoon rainfall while peak season rainfall increases, a delay and shortening of the monsoon season (Seth et al. 2013), and prolonged dry spells between the rainy events (Christensen et al., 2013). However, inter-model discrepancies are large (Yin et al., 2013). CMIP5 models also likely underestimate the climate variability of the South American monsoon and its sensitivity to climate forcing (Fu et al., 2013). Bias-corrected projections generally show a drier climate over eastern Amazonia (e.g., Duffy et al., 2015; Malhi et al., 2008). Thus, the risk of strong climatic drying and potential rainforest die-back in the future remains real.

4. Extreme precipitation events in summer monsoons

4. 1. Past changes and attribution

Over the past century, significant increases in extreme precipitation in association with global warming have emerged over the global land monsoon region as a whole, and annual maximum daily rainfall has increased at the rate of about 10-14%/°C in the southern part of the South African monsoon, about 8%/°C in the South Asian monsoon, 6-11%/°C in the NAM, and

315 15-25%/°C in the eastern part of the South American monsoon (Zhang and Zhou 2019). At Seoul,
316 Korea, one of the world's longest instrumental measurements of daily precipitation since 1778
317 shows that the annual maximum daily rainfall and the number of extremely wet days, defined as
318 the 99th percentile of daily precipitation distribution, all have an increasing trend significant at
319 the 99% confidence level (Fig. 6). In the central Indian subcontinent, a significant shift towards
320 heavier precipitation in shorter duration spells occurred from 1950–2015 (Fig. 7) (Roxy et al. 2017,
321 Singh et al. 2019). In East Asia, the average extreme rainfall trend increased from 1958 to 2010,
322 with a decreasing trend in northern China that was offset by a much larger increasing trend in
323 southern China (Chang et al. 2012). Over tropical South America, extreme indices such as annual
324 total precipitation above the 99th percentile and the maximum number of consecutive dry days
325 display more significant and extensive trends (Skansi et al. 2013, Hilker et al. 2014).

326 Attribution studies show that global warming has already increased the frequency of
327 heavy precipitation since the mid-20th Century. An optimal fingerprinting analysis shows that
328 anthropogenic forcing has made a detectable contribution to the observed shift towards heavy
329 precipitation in eastern China (Ma et al. 2017). Simulations with all and natural-only forcing show
330 that global warming increased the probability of the 2016 Yangtze River extreme summer rainfall
331 by 17%–59% (Yuan et al. 2018). A large ensemble experiment also showed that historical global
332 warming has increased July maximum daily precipitation in western Japan (Kawase et al. 2019).

333 Another anthropogenic forcing is urbanization. A significant correlation between rapid
334 urbanization and increased extreme hourly rainfall has been detected in the Pearl River Delta and
335 Yangtze River Delta of coastal China (Fig. 8) (Wu et al. 2019, Jiang et al. 2019). The increasing
336 trends are larger in both extreme hourly rainfall and surface temperature at urban stations than

those at nearby rural stations. The correlation of urbanization and extreme rainfall is due to the urban heat island effect, which increases instability and facilitates deep convection. Large spatial variability in the trends of extreme rainfall in India due to urbanization and changes in land-use and land-cover has also been detected (Ali and Mishra 2017).

Land-falling tropical cyclones (TCs) make large contributions to heavy precipitation in coastal East Asia. In the last 50 years, the decreasing frequency of incoming western North Pacific (WNP) TCs more than offsets the increasing TC rainfall intensity, resulting in reduced TC-induced extreme rainfall in southern coastal China, so the actual increase in non-TC extreme rainfall is even larger than observed (Chang et al. 2012). Evidence in the WNP, and declining TC landfall in eastern Australia (Nicholls et al. 1998), suggest that this poleward movement reflects greater poleward TC recurvature.

4.2. Future Projection

One of the most robust signals of projected future change is the increased occurrence of heavy rainfall on daily-to-multiday time scales and intense rainfall on hourly time scales. Heavy rainfall will increase at a much larger rate than the mean precipitation, especially in Asia (Kitoh, 2013, 2017). Unlike mean precipitation changes, heavy and intense rainfall is more tightly controlled by the environmental moisture content related to the Clausius-Clapeyron relationship and convective-scale circulation changes. On average, extreme five-day GM rainfall responds approximately linearly to global temperature increase at a rate of 5.17 (4.14–5.75)%/°C under RCP8.5 with a high signal-to-noise ratio (Zhang et al. 2018). Regionally, extreme precipitation in the Asian monsoon region exhibits the highest sensitivity to warming, while changes in the North American and Australian monsoon regions are moderate with low signal-to-noise ratio (Zhang et

al. 2018). CMIP6 models project changes of extreme 1-day rainfall of +58% over South Asia and +68% over East Asia in 2065–2100 compared to 1979–2014 under the SSP2-4.5 scenario (Ha et al. 2020b). Model experiments also indicate a three-fold increase in the frequency of rainfall extremes over the Indian subcontinent under future projections for global warming of 1.5°C–2.5°C (Bhowmick et al. 2019). Meanwhile, light-to-moderate rain events may become less frequent (Sooraj et al. 2016).

Changes in the variability of monsoon rainfall may occur on a range of time scales. Brown et al. (2017) found increased rainfall variability under RCP8.5 for each time scale from daily to decadal over the Australian, South Asian, and East Asian monsoon domains (Fig. 8). The largest fractional increases in monsoon rainfall variability occur for South Asian at all sub-annual time scales and for the East Asian monsoon at annual-to-decadal time scales. Future changes in rainfall variability are significantly positively correlated with changes in mean wet season rainfall for each of the monsoon domains and for most time scales.

Selected CMIP5 models project more severe floods and droughts in the future climate over South Asia (Sharmila et al. 2015; Singh et al. 2019). Due to more rapidly rising evaporation, the projections for 2015–2100 under CMIP6 SSP2-4.5 and SSP5-8.5 scenarios indicate that the western part of East Asia will confront more rapidly increasing drought severity and risks than the eastern part (Ha et al. 2020b).

Projections of future extreme rainfall change in the densely populated and fast-growing coastal zones are particularly important for several reasons. First, in fast-growing urban areas, extreme rainfall will likely intensify in the future, depending on the economic growth of the affected areas. Second, future extreme rainfall changes in coastal areas will be affected by future

changes in landfalling TCs. For instance, TC projections (Knutson et al. 2019b) suggest a continued (albeit with lower confidence) northward trend. Assuming this means more recurvature cases, it would lead to extreme rainfall increases in coastal regions of Korea and Japan and decreases in China. Third, the increase in monsoon extreme rains and TCs, together with rising sea level will lead to aggravated impacts, for instance, along coastal regions of the Indian subcontinent (Collins et al. 2019).

5. Model Issues and Future Outlook

5.1 Major common issues and missing processes

CMIP6 models improve the simulation of present-day solstice season precipitation climatology and the GM precipitation domain and intensity over the CMIP5 models; and CMIP6 models reproduce well the annual cycle of the NH monsoon and the leading mode of GM interannual variability and its relationship with ENSO (Wang et al. 2020). However, the models have major common biases in equatorial oceanic rainfall and SH monsoon rainfall, including overproduction of annual mean SH monsoon precipitation by more than 20%, and the simulated onset is early by two pentads while the withdrawal is late by 4-5 pentads (Wang et al. 2020). Systematic model biases in monsoon climates have persisted through generations of CMIP (e.g., Sperber et al., 2013). In particular, the poor representation of precipitation climatology is seen in many regional monsoons, such as Africa (Creese and Washington 2016, Han et al. 2019), and North America (Geil et al., 2013). These biases are often related to SST biases in adjacent oceans (Cook and Vizy 2013, Pascale et al., 2017). There are additional outstanding common issues for regional monsoon simulations, which are not immediately apparent in quick-look analyses. A major one is the diurnal cycle, which is poorly simulated in the tropics, due to failures in

convective parameterization (Willetts et al., 2017). Biases in evapotranspiration also affect the Bowen ratio (Yin et al. 2013), and thus atmospheric boundary layer humidity and height. Biases in variability emerge in historical monsoon simulations, hampering accurate attribution of present-day monsoon changes (Herman et al. 2019; Marvel et al, 2019) and amplifying uncertainties in future projections.

While there are subtle improvements from CMIP3 to CMIP5 and to CMIP6 due to steady increases in horizontal resolution and improved parameterizations, simulation of monsoon rainfall is still hampered by missing or poorly resolved processes. These include the lack of organized convection (e.g., mesoscale convective systems or monsoon depressions) at coarse model resolutions, poorly simulated orographic processes, and imperfect land-atmosphere coupling due to under-developed parametrizations and a paucity of observations of land-atmosphere exchanges that can only be improved through field observation programs (e.g. Turner et al., 2019). Further, proper simulation of how aerosols modify monsoon rainfall requires improved cloud microphysics schemes (Yang et al., 2017; Chu et al., 2018). Finally, some features of monsoon meteorology that are crucial to climate projection and adaptation, such as extreme rainfall accumulations exceeding 1 meter/day, are nearly impossible to simulate in coupled climate models. High-resolution regional simulations can potentially ameliorate biases, but they still must rely on GCM-generated boundary conditions in their projections. Convection-permitting regional simulations have been suggested to more realistically represent short time scale rainfall processes and their responses to forcing (e.g. in future simulations for Africa; Kendon et al., 2019).

5.2 Sources of model uncertainty in future projection of monsoons

425 The major sources of projection uncertainty include model uncertainty, scenario
426 uncertainty and internal variability. Contributions from internal variability decrease with time,
427 while those from scenario uncertainty increase. Model uncertainty dominates near-term
428 projections of GM mean and extreme precipitation with a contribution of ~90% (Zhou et al.
429 2020a). Model uncertainty often arises from divergent circulation changes. In particular,
430 circulation changes caused by regional SST warming and land-sea thermal contrast can generally
431 contribute to uncertainty in monsoon rainfall changes (Chen and Zhou, 2015; Pascale et al., 2017).
432 Uncertainty in projected surface warming patterns is closely related to present-day model biases,
433 including the cold-tongue bias in the tropical eastern Pacific (Chen and Zhou, 2015; Ying et al.
434 2019) and a cold bias beneath underestimated marine stratocumulus, which can induce a large
435 land-sea thermal contrast in the future (Nam et al. 2012, Chen et al. 2019). Monsoons are
436 strongly influenced by cloud and water vapor feedbacks (Jalihal et al., 2019; Byrne and Zanna,
437 2020), yet how the large variations in these feedbacks across climate models impact monsoon
438 uncertainties is unknown. Another factor affecting future monsoon changes are vegetation
439 feedbacks. Cui et al. (2019) showed that they may exacerbate the effects of CO2-induced
440 radiative forcing, especially in the North and South American and Australian monsoons via
441 reduced stomatal conductance and transpiration. Vegetation is an important water vapor
442 provider and can affect monsoon onsets (Wright et al. 2017; Sori et al. 2017), yet current climate
443 models have limited capability in representing how vegetation responds to climate and elevated
444 CO_2, and how land use and fires affect future vegetation distribution and functions. The extent
445 to which these model limitations contribute to the uncertainty of future monsoon rainfall
446 projections is virtually unknown, although plant physiological effects may exacerbate CO2-

447 raditiative impacts (Cui et al., 2019). While CMIP6 models are more advanced in terms of physical
448 processes included and resolution, the inter-model spread in projection of monsoons in CMIP6
449 models has remained as large (or became larger) compared to CMIP5 models (Fig 2).

450 5.3 Future Outlook

451 Future models might improve by explicitly resolving deep convection to address common
452 problems across monsoon systems. In attribution, controversies remain over the relative roles of
453 natural multidecadal variability and anthropogenic forcing, especially of aerosol effects on the
454 observed historical monsoon evolution in Asia and West Africa. Quantification of the roles of
455 multidecadal variability in biasing the transient climate sensitivity in observations as well as in
456 model simulations is encouraged.

457 There is an urgent need to better understand sources of uncertainty in future rainfall
458 projections. Such sources encompass but are not limited to structural uncertainty, uncertainties
459 in aerosol processes and radiative forcing, the roles of internal modes of variability and their
460 potential changes in the future, ecosystem feedbacks to climate change and elevated CO_2, and
461 land-use impacts. To have more confidence in future projections, we need to quantify the causes
462 of spread in future climate signals at the process level: the relative magnitudes of forcing
463 uncertainty versus mean-state biases and feedback uncertainties. This type of error
464 quantification requires specially designed, coordinated simulations across modelling centers and
465 a focus on the key processes that need to be improved.

466 Traditional future assessments of the global monsoon continue to rely on multi-model
467 approaches. However, a small multi-model ensemble such as CMIP5 or CMIP6 may not represent
468 the full extent of uncertainty introduced by internal (multi-decadal) variability. More recently,

large ensembles are being employed to help understand the spread or degree of uncertainty in a climate signal, and, at the regional level, the interplay between internal variability and anthropogenic external forcing in determining a climate anomaly. Such large ensembles are either perturbed-parameter ensembles (PPE) (Murphy et al., 2014) or alternatively, traditional initial-condition ensembles – e.g., by CanESM2 (Sigmond and Fyfe, 2016; Kirchmeier-Young, 2017) or by MPI-ESM (Maher et al., 2019) – with tens to a hundred members. Large-ensemble methods should be applied to the global monsoon in order to determine the extent to which internal variability can explain its declining rainfall in the late 20th century. We suggest that an additional pathway to more reliable monsoon projections would be to develop emergent constraints applicable to monsoons, and this should be a focus for the research community.

Recent theoretical advances in tropical atmospheric dynamics offer new avenues to further our understanding of monsoon circulations in a changing climate. Monsoon locations have been shown to coincide with maxima in sub-cloud moist static energy (MSE) (Privé and Plumb 2007), with MSE budgets likely to be useful for understanding the response of monsoons to external forcing (Hill 2019). Recent studies of the ITCZ may also provide new insights into the strength and spatial extent of monsoons. Theoretical work has identified energetic (Sobel and Neelin, 2006; Byrne and Schneider, 2016) and dynamical constraints (Byrne and Thomas, 2019) on the width of the ITCZ, with implications for its strength (Byrne et al., 2018). Additionally, Singh et al. (2017) have linked the strength of the Hadley circulation to meridional gradients in moist entropy. The extent to which these theories can explain CMIP6 changes in monsoon strength and spatial extent is an open question that should be prioritized.

Understanding past monsoon responses to external forcings may shed light on future climate change. The NH monsoon future response is shown to be weaker than in simulations of the mid-Holocene, although future warming is larger (D'Agostino et al. 2019). This occurs because both thermodynamic and dynamic responses act in concert and cross-equatorial energy fluxes shift the ITCZ towards the warmer NH during the mid-Holocene, but in the future, they partially cancel. The centennial-millennial variations of GM precipitation before the industrial period are mainly attributable to solar and volcanic (SV) forcing (Liu et al., 2009). For the same degree of warming, GHG forcing induces less rainfall increase than SV forcing because the former increases stability, favoring a weakened Walker circulation and El Niño-like warming, while the latter warms tropical Pacific SSTs in the west more than the east, favoring a La Nina-like warming through the ocean thermostat mechanism (Liu et al. 2013). An El Niño-like warming reduces GM precipitation (Wang et al. 2012). Jalihal et al. (2019), by examining responses of tropical precipitation to orbital forcing, find that the changes in precipitation over land are mainly driven by changes in insolation, but over the oceans, surface fluxes and vertical stability play an important role in precipitation changes.

6. Summary

We have reviewed past monsoon changes and their primary drivers, summarized projected future changes and key physical processes, and discussed challenges of the present and future modeling and outlooks. In this section we will assign a level of confidence to the main conclusions wherever feasible.

1. Extreme rainfall events.

Continued global warming over the past century has already caused a significant rise in the intensity and frequency of extreme rainfall events in all monsoon regions (e.g., Figs. 6 and 7; high

512 confidence). Urbanization presents additional anthropogenic forcing that significantly increases localized
513 extreme rainfall events in areas of rapid economic growth due to the urban heat island effect (Fig. 8, high
514 confidence). This urban effect is expected to expand to more locations with the growing economy,
515 especially in Asia. There is some indication that TC tracks in the western North Pacific have been shifting
516 more towards the recurvature type. If this trend continues, it may cause an increase in the ratio of TC-
517 related extreme rainfall in Korea and Japan versus China (low confidence).

518 Almost all future projections agree that the frequency and intensity of extreme rainfall events will
519 increase. The occurrence of heavy rainfall will increase on daily-to-multiday time scale and intense rainfall
520 on hourly time scales. The increased extreme rainfall is largely due to an increase in available moisture
521 supply and convective-scale circulation changes. Meanwhile, models also project prolonged dry spells
522 between the heavy rainy events, which, along with enhanced evaporation and runoff of ground water
523 during heavy rainfall, will lead to an increased risk of droughts over many monsoon regions (high
524 confidence). Notably, the enhanced extreme rain events will *likely* contribute to compound events—
525 where increasing tropical cyclones, rising sea level, and changing land conditions—may aggravate the
526 impact of floods over the heavily populated coastal regions.

527 *2. Mean monsoon rainfall and its variability*

528 Observed changes in the mean monsoon rainfall vary by region with significant decadal variations
529 that have been related to internal modes of natural variability. Since the 1950s, NH anthropogenic
530 aerosols may be a significant driver in the Sahel drought and decline of monsoon rainfall in South Asia
531 (medium-high confidence). NH land monsoon rainfall as a whole declined from 1950 to 1980 and
532 rebounded after the 1980s, due to the competing influence of internal climate variability, radiative forcing
533 from GHGs and aerosol forcing (high confidence); however, it remains a challenge to quantify their relative
534 contributions. CMIP6 historical simulations suggest that anthropogenic sulfate and volcanic forcing likely

masked the effect of GHG forcing and caused the downward trend from 1950 to 1990 (Fig. 2); however, the recent upward trend may signify the emergence of the greenhouse-gas signal against the rainfall reduction due to aerosol emissions (medium-high confidence).

CMIP6 models project a larger increase in monsoon rainfall over land than over ocean (Fig. 2). Land monsoon rainfall will likely increase in the NH, but change little in the SH (Figs. 2 and 4). Regionally, land monsoon rainfall will increase in South Asia and East Asia (high confidence), and northern Africa (medium confidence), but decrease over North American monsoon region (high confidence) (Fig. 3). The projected mean rainfall changes (either neutral or slightly decreasing) over SH (American, Australian, and Southern African) monsoons have low confidence due to a large spread. The future change of GM precipitation pattern and intensity is determined by increased specific humidity and circulation changes forced by the vertically and horizontally inhomogeneous heating induced by GHG radiative forcing. Under GHGs-induced warming, the land monsoon rainy season changes considerably from region to region; yet, as a whole, the rainy season will likely be lengthened in the NH due to late retreat (with most significant change over East Asia), but shortened in the SH due to delayed onset. The variability of monsoon rainfall is projected to increase on daily to decadal time scales over the Asian-Australian monsoon region (Fig. 9). Models generally underestimate the magnitude of observed precipitation changes, which poses a major challenge for quantitative attributions of regional monsoon changes. The range of projected change of annual-mean global land monsoon precipitation by the end of the 21st century in CMIP6 is *likely* about 50% larger than in corresponding scenarios of CMIP5.

Acknowledgments

This work is a task of the World Meteorological Organization's (WMO) World Weather Research Programme (WWRP). All authors are invited experts by the WMO/WWRP Working Group for Tropical Meteorology Research. We wish to thank Sun Yat-sen University for hosting the WMO Workshop on Monsoon Climate Change Assessment in Zhuhai, China, in which this review was discussed. This work was supported in part by the National Natural Science Foundation of China under Grant 91637208 to Sun Yat-sen University.

References

Abbs, D., 2012: The impact of climate change on the climatology of tropical cyclones in the Australian region. *Aspendale: CSIRO,* **11,** doi:10.4225/08/584ee7d4585f5.

Aguilar, E., T. C. Peterson, P. Ramírez Obando, R. Frutos, J. A. Retana, M. Solera, J. Soley, I. González García, R. M. Araujo, A. Rosa Santos, V. E. Valle, M. Brunet, L. Aguilar, L. Álvarez, M. Bautista, C. Castañón, L. Herrera, E. Ruano, J. J. Sinay, E. Sánchez, G. I. Hernández Oviedo, F. Obed, J. E. Salgado, J. L. Vázquez, M. Baca, M. Gutiérrez, C. Centella, J. Espinosa, D. Martínez, B. Olmedo, C. E. Ojeda Espinoza, R. Núñez, M. Haylock, H. Benavides, and R. Mayorga 2005: Changes in precipitation and temperature extremes in Central America and northern South America, 1961–2003. *J. Geophys. Res.,* **110,** D23107.

Ali, H., and V. Mishra, 2017: Contrasting response of rainfall extremes to increase in surface air and dewpoint temperatures at urban locations in India. Scientific Reports, 7, 1228.

Annamalai, H., J. Hafner, K. P. Sooraj and P. Pillai, 2013: Global warming shifts the monsoon circulation, drying South Asia. J. Climate, 26, 2701-2718.

Bayr, T., D. Dommenget, T. Martin, and S. B. Power, 2014: The eastward shift of the Walker circulation in response to global warming and its relationship to ENSO variability. *Climate Dyn.,* **43,** 2747–2763, doi:10.1007/s00382-014-2091-y.

Bhowmick, M., S. Sahany, and S. K. Mishra, 2019: Projected precipitation changes over the south Asian region for every 0.5° C increase in global warming. *Environ. Res. Lett.,* **14,** 054005, doi:10.1088/1748-9326/ab1271.

Bollasina, M. A., Y. Ming, and V. Ramaswamy, 2011: Anthropogenic aerosols and the weakening of the South Asian summer monsoon. *Science,* **334,** 502-505.

Byrne, M. P., and T. Schneider, 2016: Narrowing of the ITCZ in a warming climate: physical mechanisms. *Geophys. Res. Lett.,* **43,** 350.

588 Byrne, M. P., A. G. Pendergrass, A. D. Rapp, and K. R. Wodzicki, 2018: Response of the intertropical
589 convergence zone to climate change: Location, width, and strength. *Current Climate Change*
590 *Reports,* **4,** 355–370, doi:10.1007/s40641-018-0110-5.
591 Byrne, M. P., and R. Thomas, 2019: Dynamics of ITCZ width: Ekman processes, non-Ekman processes, and
592 links to sea surface temperature. *J. Atmos. Sci.,* **76,** 2869–2884.
593 Byrne, M. P., and L. Zanna, 2020: Radiative effects of clouds and water vapor on the monsoon. *J. Climate*,
594 in revision (preprint available at https://drive.google.com/file/d/1HJgsclJlqFR_tFFVHB-
595 NxoyzJdQjJk4J/view).
596 Bukovsky, M. S., C. M. Carrillo, D. J. Gochis, D. M. Hammerling, R. R. McCrary, and L. O. Mearns, 2015:
597 Toward assessing NARCCAP Regional Climate Model credibility for the North American Monsoon:
598 future climate simulations. *J. Climate,* **28,** 6707–6728.
599 Cai, W., X.-T. Zheng, E. Weller, M. Collins, T. Cowan, M. Lengaigne, T. Yamagata, 2013: Projected response
600 of the Indian Ocean dipole to greenhouse warming. *Nature Geoscience,* **6,** 999–1007.
601 Cai, W., G. Wang, A. Santoso, M. J. McPhaden, L. Wu, F.-F. Jin, and E. Guilyardi, 2015: Increased frequency
602 of extreme La Niña events under greenhouse warming. *Nature Climate Change,* **5,** 132–137.
603 Cattani, E., A. Merino, J. A. Guijarro, and V. Levizzani, 2018: East Africa rainfall trends and variability 1983–
604 2015 using three long-term satellite products. *Remote Sensing,* **10,** 931, doi:10.3390/rs10060931.
605 Chang, C. W. J., W.-L. Tseng, H.-H. Hsu, N. Keenlyside, and B.-J. Tsuang, 2015: The Madden-Julian
606 oscillation in a warmer world. *Geophy. Res. Lett.*, *42,* 6034–6042.
607 Chang, C.-P., M. Ghil, H.C. Kuo, M. Latif, C. H. Sui, and J. M. Wallace, 2014: Understanding multidecadal
608 climate changes. *Bull. Am. Meteorol. Soc.,* **95**, 293–296. doi: 10.1175/BAMS-D-13-00015.1.
609 Chang, C.-P., Y. Lei, C.-H. Sui, X. Lin, and F. Ren, 2012: Tropical cyclone and extreme rainfall trends in East
610 Asian summer monsoon since mid-20th century, Geophys. Res. Lett., 39, L18702,
611 doi:10.1029/2012GL052945.

612 Chang, C.-P., Z. Wang, J. McBride and C. H. Liu, 2005: Annual cycle of Southeast Asia - Maritime Continent
613 rainfall and the asymmetric monsoon transition. *J. Climate,* **18**, 287-301.
614 Chen, X., and T. Zhou, 2015: Distinct effects of global mean warming and regional sea surface warming
615 pattern on projected uncertainty in the South Asian summer monsoon. *Geophys. Res. Lett.,* **42,**
616 9433–9439.
617 Chen, X., T. Zhou, P. Wu, Z. Guo, and M. Wang, 2019: Emergent constraints on future projections of the
618 western North Pacific Subtropical High. *Nat. Commun.,* under review. Manuscript is available at
619 https://drive.google.com/open?id=1hkuL4G_xQ-2B6PBYGSMHXDhBrcAARaPZ
620 Christensen, J.H., K. Krishna Kumar, E. Aldrian, S.-I. An, I.F.A. Cavalcanti, M. de Castro, W. Dong, P.
621 Goswami, A. Hall, J.K. Kanyanga, A. Kitoh, J. Kossin, N.-C. Lau, J. Renwick, D.B. Stephenson, S.-P.
622 Xie and T. Zhou, 2013: Climate Phenomena and their Relevance for Future Regional Climate
623 Change. In: Climate Change 2013: The Physical Science Basis. Contribution of Working Group I to
624 the Fifth Assessment Report of the Intergovernmental Panel on Climate Change [Stocker, T.F., D.
625 Qin, G.-K. Plattner, M. Tignor, S.K. Allen, J. Boschung, A. Nauels, Y. Xia, V. Bex and P.M. Midgley
626 (eds.)]. Cambridge University Press, Cambridge, United Kingdom and New York, NY, USA.
627 Chu, J.-E., K.-M. Kim, W. K. M. Lau and K.-J. Ha, 2018: How light absorbing properties of organic aerosol
628 modify the Asian summer monsoon rainfall? *J. Geophys. Res. Atmos.,* **123,** 2244–2255,
629 doi:10.1002/2017JD027642.
630 Collins, M., and Coauthors, 2019: Extremes, Abrupt Changes and Managing Risk, in Portner et al., eds.
631 IPCC Special Report on Oceans and Cryosphere in a Changing Climate. Cambridge University Press,
632 Cambridge, United Kingdom and New York, NY, USA.
633 Cook, B. I. and R. Seager, 2013: The response of the North American Monsoon to increased greenhouse
634 gas forcing. *J. Geophys. Res.,* **118,** 1690–1699.

635 Cook, K. H., and E. K. Vizy, 2013: Projected changes in East African rainy seasons. *J. Climate,* **26,** 5931–
636 5948, doi:10.1175/JCLI-D-12-00455.1
637 Cook, K. H., and E. K. Vizy, 2019: Congo Basin drying associated with poleward shifts of African thermal
638 lows. *Climate Dyn.,* doi:10.1007/s00382-019-05033-3.
639 Creese, A., and R. Washington, 2016: Using qflux to constrain modeled Congo Basin rainfall in the CMIP5
640 ensemble. *J. Geophys. Res.,* **121,** 13415–13442, doi:10.1002/2016JD025596.
641 Cui, J., S. Piao, C. Huntingford, X. Wang, X. Lian, A. Chevuturi, A. G. Turner and G. J. Kooperman, 2019:
642 Vegetation forcing modulates global land monsoon and water resources in a CO2-enriched
643 climate. Nature Geosciences, submitted. The latest version of this paper is available at:
644 https://livereadingac-my.sharepoint.com/:f:/g/personal/a_g_turner_reading_ac_uk/
645 El8hjGgHjs5KooEbLEP0lIIBGgSajLIwumjN9ARCV7lJNQ?e=GrH4NI
646 D'Agostino, R., J. Bader, S. Bordoni, D. Ferreira, and J. Jungclaus, 2019: Northern Hemisphere monsoon
647 response to mid-Holocene orbital forcing and greenhouse gas-induced global warming. *Geophys.*
648 *Res. Letts.,* **46,** 1591–1601, doi:10.1029/2018GL081589.
649 Deser, C., A. S. Phillips, and M. A. Alexander, 2010: Twentieth century tropical sea surface temperature
650 trends revisited. *Geophys. Res. Lett.,* **37,** L10701.
651 Dey, R., S. C. Lewis, J. M. Arblaster, and N. J. Abram, 2019: A review of past and projected changes in
652 Australia's rainfall. *Wiley Interdiscip. Rev. Clim. Chang.,* **10,** 1–23, doi:10.1002/wcc.577.
653 Ding, Y., Y. Sun, Z. Wang, Y. Zhu, and Y. Song, 2009: Inter-decadal variation of the summer precipitation in
654 China and its association with decreasing Asian summer monsoon Part II: Possible causes, Int. J.
655 Climatology, 29, 1926-1944.
656 Dong, B., L. J. Wilcox, E. J. Highwood, and R. T. Sutton, 2019: Impacts of recent decadal changes in Asian
657 aerosols on the East Asian summer monsoon: roles of aerosol–radiation and aerosol–cloud
658 interactions. *Climate Dyn.,* **53,** 3235, doi:10.1007/s00382-019-04698-0.

659 Duffy, P. B., P. Brando, G. P. Asner, and C. B. Field, 2015: Projections of future meteorological drought and
660 wet periods in the Amazon. *Proc. Natl. Acad. Sci. USA,* **112,** 13172–13177,
661 doi:10.1073/pnas.1421010112.
662 Endo, H., A. Kitoh, T. Ose, R. Mizuta, and S. Kusunoki, 2012: Future changes and uncertainties in Asian
663 precipitation simulated by multiphysics and multi–sea surface temperature ensemble
664 experiments with high-resolution Meteorological Research Institute atmospheric general
665 circulation models (MRI-AGCMs). *J. Geophys. Res.,* **117,** D16118, doi:10.1029/2012JD017874.
666 Endo, H., and A. Kitoh, 2014: Thermodynamic and dynamic effects on regional monsoon rainfall changes
667 in a warmer climate. *Geophys. Res. Lett.,* **41,** 1704–1711.
668 Endo, H., A. Kitoh, and H. Ueda, 2018: A unique feature of the Asian summer monsoon response to global
669 warming: the role of different land–sea thermal contrast change between the lower and upper
670 troposphere. *SOLA*, **14,** 57–63, doi:10.2151/sola.2018-010.
671 Fu, R., L. Yin, W. Li, P. A. Arias, R. E. Dickinson, L. Huang, S. Chakraborty, K. Fernandes, B. Liebmann, R.
672 Fisher, and R. B. Myneni, 2013: Increased dry-season length over southern Amazonia in recent
673 decades and its implication for future climate projection. *Proc. Natl. Acad. Sci. USA,* **110,** 18110–
674 18115, doi:10.1073/pnas.1302584110.
675 Geil, K. L., Y. L. Serra, and X. Zeng, 2013: Assessment of CMIP5 Model Simulations of the North American
676 Monsoon System. *J. Climate,* **26,** 8787–8801, doi:10.1175/JCLI-D-13-00044.1.
677 Giannini, A, and A. Kaplan, 2019: The role of aerosols and greenhouse gases in Sahel drought and recovery.
678 *Climatic Change*, 152, 449-466.
679 Gonzalez, P. L. M., L. M. Polvani, R. Seager, G. J. Correa, 2014: Stratospheric ozone depletion: a key driver
680 of recent precipitation trends in South Eastern South America. *Climate Dyn.,* **42,** 1775–1792.
681 Goswami, B. N., V. Venugopal, D. Sengupta, M. Madhusoodanan, and P. K. Xavier, 2006: Increasing trend
682 of extreme rain events over India in a warming environment. *Science,* **314,** 1442–1445.

683 Grimm, A. M., J. Pal, and F. Giorgi, 2007: Connection between spring conditions and peak summer
684 monsoon rainfall in South America: Role of soil moisture, surface temperature, and topography
685 in eastern Brazil. *J. Climate,* **20,** 5929-5945.
686 Grimm, A. M., 2011: Interannual climate variability in South America: impacts on seasonal precipitation,
687 extreme events and possible effects of climate change. *Stochastic Environmental Research and*
688 *Risk Assessment*, 25, 537-554, DOI: 10.1007/s00477-010-0420-1
689 Grimm, A. M., and J. P. J. Saboia, 2015: Interdecadal variability of the South American precipitation in the
690 monsoon season. *J. Climate,* **28,** 755-775, doi:10.1175/JCLI-D-14-00046.1.
691 Ha, K. J., B. H. Kim, E. S. Chung, J. C. L. Chan, and C. P. Chang, 2020a: Major factors of monsoon rainfall
692 changes:natural versus anthropogenic forcing. *Environ. Res. Lett.,* doi:10.1088 /1748-9326/ab7767.
693 Ha, K. J., S. Moon, D. Kim, A. Timmermann, and D. Kim, 2020b: Future changes of summer monsoon
694 characteristics and evaporative demand over Asia in CMIP6 simulations. Geophys. Res. Lett.,
695 doi:10.1029/2020GL087492.
696 Han, F., K. H. Cook, E. K. Vizy, 2019: Changes in intense rainfall events and drought across Africa in the
697 21st century. *Climate Dyn.,* 53, 2757-2777. doi:10.1007/s00382-019-04653-z.
698 He, B., S. Yang, and Z. Li, 2016: Role of atmospheric heating over the South China Sea and western Pacific
699 regions in modulating Asian summer climate under the global warming background. Climate Dyn.,
700 46, 2897-2908.
701 He, S., S. Yang, and Z. Li, 2017: Influence of latent heating over the Asian and western Pacific monsoon
702 region on Sahel summer rainfall. Sci. Reports, 7, 7680, https://doi.org/10.1038/s41598-017-
703 07971.
704 Held, I. M. and B. J. Soden, 2006: Robust responses of the hydrological cycle to global warming. *J. Climate,*
705 **19,** 5686–5699.

706 Herman, R. J., A. Giannini, M. Biasutti, and Y. Kushnir, 2019: The Effects of Anthropogenic and Volcanic
707 Aerosols and Greenhouse Gases on 20th Century Sahel Precipitation. *Scientific Reports,* submitted.
708 Hilker, T., A. I. Lyapustin, C. J. Tucker, F. G. Hall, R. B. Myneni, Y. Wang, J. Bi, Y. M. de Moura, and P. J.
709 Sellers, 2014: Vegetation dynamics and rainfall sensitivity of the Amazon. *Proc. Natl. Acad. Sci.*
710 *USA,* **111,** 16041–16046, doi:10.1073/pnas.1404870111
711 Hill, S. A., 2019: Theories for Past and Future Monsoon Rainfall Changes. *Current Climate Change Reports,*
712 **5,** 160-171.
713 Hsu, P.-C., T. Li, H. Murakami and A. Kitoh, 2013: Future change of the global monsoon revealed from 19
714 CMIP5 models. *J. Geophys. Res. Atmos.,* **118,** 1247–1260.
715 Huang, P., S.-P. Xie, K. Hu, G.Huang and R. Huang, 2013: Patterns of the seasonal response of tropical
716 rainfall to global warming, Nature Geos., 6, 357-361.
717 Huang, X., T. Zhou, A. Dai, H. Li, C. Li, X. Chen, J. Lu, J.-S. von Storch, and B. Wu, 2020a: South Asian summer
718 monsoon projections constrained by the Interdecadal Pacific Oscillation. *Science Advances,6,*
719 *eaay6546*. DOI: 10.1126/sciadv.aay6546.
720 Huang, X., T. Zhou, A. Turner, A. Dai, X. Chen, R. Clark, J. Jiang, W. Man, J. Murphy, J. Rostron, B. Wu, L.
721 Zhang, W. Zhang, and L. Zou, 2020b: The recent decline and recovery of Indian summer monsoon
722 rainfall: relative roles of external forcing and internal variability. *J. Climate,* Accepted 12 March
723 2020. doi: 10.1175/JCLI-D-19-0833.1
724 Huang, X., T. Zhou, W. Zhnag, J. Jiang, P. Li, Y. Zhao, 2019: Northern Hemipshere land monsoon
725 precipitation chnages in the twentieth century revealed by multple Reanalysis datasets, Climate
726 Dyn., https://doi.org/10.1007/s00382-019-04982-z
727 Jalihal, C., J. Srinivasan, and A. Chakraborty, 2019: Modulation of Indian monsoon by water vapor and
728 cloud feedback over the past 22,000 years. *Nature Communications,* **10,** 1–8,
729 doi:10.1038/s41467-019-13754-6.

730 Jiang, X., Y. Luo, D.-L. Zhang, and M. Wu, 2019: Urbanization Enhanced Summertime Extreme Hourly
731 Precipitation over the Yangtze River Delta, J Climate, Revised version submitted.
732 Jiang Jie, Tianjun Zhou. 2019. Global monsoon responses to decadal sea surface temperature variations
733 during the twentieth century: Evidence from AGCM simulations. *Journal of Climate*, doi:
734 10.1175/JCLI-D-18-0890.1
735 Jin, Q., Wang, C. A revival of Indian summer monsoon rainfall since 2002. *Nature Clim Change* **7,** 587–594
736 (2017).
737 Jourdain, N. C., A. S. Gupta, A. S. Taschetto, C. C. Ummenhofer, A. F. Moise, and K. Ashok, 2013: The Indo-
738 Australian monsoon and its relationship to ENSO and IOD in reanalysis data and the CMIP3/CMIP5
739 simulations. *Climate Dyn.,* **41,** 3073–3102, doi:10.1007/s00382-013-1676-1.Kawase, H., A. Murata,
740 R. Mizuta, H. Sasaki, M. Nosaka, M. Ishii, and I. Takayabu, 2016: Enhancement of heavy daily
741 snowfall in central Japan due to global warming as projected by large ensemble of regional climate
742 simulations. Climatic Change, 139, 265-278, doi:10.1007/s10584-016-1781-3.
743 Kawase, H., Y. Imada, H. Sasaki, T. Nakaegawa, A. Murata, M. Nosaka, and I. Talayabu, 2019: Contribution
744 of historical global warming to local-scale heavy precipitation in western Japan estimated by large
745 ensemble high-resolution simulations. J. Geophys. Res. Atmos., 124, 6093-6103,
746 doi:10.1029/2018JD030155.
747 Kendon, E.J., Stratton, R.A., Tucker, S. *et al.* , 2019: Enhanced future changes in wet and dry extremes over
748 Africa at convection-permitting scale. *Nat Commun* **10,** 1794. https://doi.org/10.1038/s41467-
749 019-09776-9
750 Kirchmeier-Young, M. C., F. W. Zwiers, and N. P. Gillett, 2017: Attribution of Extreme Events in Arctic Sea
751 Ice Extent. *J. Climate,* **30,** 553–571.

752 Kitoh, A., H. Endo, K. Krishna Kumar, I. F. A. Cavalcanti, P. Goswami, and T. Zhou, 2013: Monsoons in a
753 changing world: a regional perspective in a global context. *J. Geophys. Res.,* **118,** 3053–3065,
754 doi:10.1002/jgrd.50258.
755 Kitoh, A., 2017: The Asian monsoon and its future change in climate models: a review. *J. Meteor. Soc.*
756 *Japan,* **95,** 7-33, doi:10.2151/jmsj.2017-002.
757 Knutson et al. 2019a: Tropical Cyclones and Climate Change Assessment: Part I. Detection and Attribution.
758 Bull. Amer. Meteorol. Soc. doi.org/10.1175/BAMS-D-18-0189.1
759 Knutson et al. 2019b: Tropical Cyclones and Climate Change Assessment: Part II. Projected Response to
760 Anthropogenic Warming. Bull. Amer. Meteorol. Soc. doi.org/10.1175/BAMS-D-18-0194.1
761 Krishnan, R., T.P. Sabin, D.C. Ayantika, A. Kitoh, M. Sugi, H. Murakami, A.G. Turner, J.M. Slingo and K.
762 Rajendran, 2013: Will the South Asian monsoon overturning circulation stabilize any further?
763 Clim.Dyn., 40, 187–211.
764 Krishnan, R., T. P. Sabin, R. Vellore, M. Mujumdar, J. Sanjay, B. N. Goswami, F. Hourdin, J.-L. Dufresne, and
765 P. Terray, 2016: Deciphering the desiccation trend of the South Asian monsoon hydroclimate in a
766 warming world. *Climate Dyn.,* **47,** 1007–1027.
767 Lahmers, T. M., C. L. Castro, D. K. Adams, Y. L. Serra, J. J. Brost, and T. Luong, 2016: Long-term changes in
768 the climatology of transient inverted troughs over the North American monsoon region and their
769 effects on precipitation. *J. Climate,* **29,** 6037–6064.
770 Lau, W. K.-M., and K.-M. Kim, 2017: Competing influences of greenhouse warming and aerosols on Asian
771 summer monsoon circulation and rainfall, *Asia-Pac., J. Atmos. Sci.,* **53,** 181–194.
772 Lee, J.-Y. and B. Wang, 2014: Future change of global monsoon in the CMIP5. *Climate Dyn.,* **42,** 101–119,
773 doi:10.1007/s00382-012-1564-0.

774 Lee, J.-Y., K.-S. Yun, Y.-M. Yang, E.-S. Chung and A. Babu, 2019: Challenges in constraining future change
775 of global land precipitation in CMIP6 models. Presented at the WMO Workshop on Monsoon
776 Climate Change Assessment, 2-3 December 2019, Zhuhai, China.
777 Li, G., S.-P. Xie, Y. Du, and Y. Luo, 2016: Effects of excessive equatorial cold tongue bias on the projections
778 of tropical Pacific climate change. Part I: the warming pattern in CMIP5 multi-model ensemble.
779 *Climate Dyn.,* **47,** 3817–3831.
780 Li, J., and B. Wang, 2018: Origins of the decadal predictability of East Asian land summer monsoon
781 rainfall. *J. Climate,* **31,** 6229–6243.
782 Li, J., Z. Wu, Z. Jiang, and J. He, 2010: Can global warming strengthen the East Asian summer monsoon? *J.*
783 *Climate*, **23**, 6696-6705.
784 Li, W., Fu, R., 2006: Influence of cold air intrusions on the wet season onset over Amazonia. *J. Climate,* **19,**
785 257–275, doi:10.1175/JCLI3614.1.
786 Li, X., J. Yu, and Y. Li, 2013: Recent Summer Rainfall Increase and Surface Cooling over Northern Australia
787 since the Late 1970s: A Response to Warming in the Tropical Western Pacific. *J. Climate,* **26,** 7221–
788 7239, doi:10.1175/JCLI-D-12-00786.1.
789 Li, Z., W. K. M. Lau, V. Ramanathan, et al., 2016: Aerosol and monsoon climate interactions over
790 Asia. Reviews of Geophysics, 54(1-4), 866-929.
791 Li, Z., Y. Sun, T. Li, Y. Ding, and T. Hu, 2019: Future changes in East Asian summer monsoon circulation and
792 precipitation under 1.5° C to 5° C of warming. *Earth's Future,* accepted.
793 Liebmann, B., M. P. Hoerling, C. Funk, I. Bladé, R. M. Dole, D. Allured, X. Quan, P. Pegion, and J. K. Eischeid,
794 2014: Understanding recent Horn of Africa rainfall variability and change. *J. Climate,* **27**, 8629–
795 8645, doi:10.1175/JCLI-D-13-00714.1.

796 Lin, L., Z. Wang, Y. Xu, Q.Fu, and W. Dong, 2018: Larger Sensitivity of Precipitation Extremes to Aerosol
797 Than Greenhouse Gas Forcing in CMIP5 Models. *J. Geophys. Res. Atmos.,* **123,** 8062–8073.
798 doi:10.1029/2018JD028821.
799 Liu, J., B. Wang, Q. H. Ding, X. Y. Kuang, W. Soon, and E. Zorita, 2009: Centennial variations of the global
800 monsoon precipitation in the last millennium: results from ECHO-G model. *J. Climate,* **22,** 2356–
801 2371, doi:10.1175/2008JCLI2353.1.
802 Liu, J., B. Wang, M. A. Cane, S.-Y. Yim and J.-Y. Lee, 2013: Divergent global precipitation changes induced
803 by natural versus anthropogenic forcing. *Nature,* **493,** 656–659.
804 Lodoun, T., A. Giannini, P. S. Traoré, L. Somé, M. Sanon, M. Vaksmann, and J. M. Rasolodimby, 2013:
805 Changes in seasonal descriptors of precipitation in Burkina Faso associated with late 20th century
806 drought and recovery in West Africa. *Environmental Development,* **5,** 96–108.
807 Luong, T. M., C. L. Castro, H.-I Chang, T. Lahmers, D. K. Adams, and C. A. Ochoa-Moya, 2017: The more
808 extreme nature of North American monsoon precipitation in the southwestern U.S. as revealed
809 by a historical climatology of simulated severe weather events. *J. Appl. Meteor. Climatol.,* **56,**
810 2509–2529.
811 Ma, S., T. Zhou, D. A. Stone, D. Polson, A. Dai, P. A. Stott, H. von Storch, Y. Qian, C. Burke, P. Wu, L. Zou,
812 and A. Ciavarella, 2017: Detectable anthropogenic shift toward heavy precipitation over eastern
813 China. J. Climate, 30, 1381-1396.
814 Maher, N. and Coauthors, 2019: The Max Planck Institute Grand Ensemble: Enabling the exploration of
815 climate system variability. *J. Advances in Modeling Earth Systems,* **11,** 2050–2069.
816 Maidment, R. I., R. P. Allan, and E. Black, 2015: Recent observed and simulated changes in precipitation
817 over Africa. *Geophys. Res. Lett.,* **42,** 8155–8164, doi:10.1002/2015GL065765.
818 Malhi, Y., J. T. Roberts, R. A. Betts, T. J. Killeen, W. Li, and C. A. Nobre, 2008: Climate change, deforestation,
819 and the fate of the Amazon. *Science,* **319,** 169–172, doi:10.1126/science.1146961.

Maloney, E.D., Adames, Á.F. & Bui, H.X. Madden–Julian oscillation changes under anthropogenic warming. *Nature Clim Change* **9,** 26–33 (2019). https://doi.org/10.1038/s41558-018-0331-6

Marvel, K., M. Biasutti, and C. Bonfils, 2019: Fingerprints of external forcing agents on Sahel rainfall. *Environ. Res. Lett.,* revised version submitted and available for download in the ESSOAr repository: https://doi.org/10.1002/essoar.10502593.1

Moon, S., and K. J. Ha, 2017: Temperature and precipitation in the context of the annual cycle over Asia: Model evaluation and future change. *Asia-Pacific J. Atmos. Sci.,* **53,** 229–242, doi:10.1007/s13143-017-0024-5.

Murphy, J. M., B. B. Booth, C. A. Boulton, R. T. Clark, G. R. Harris, J. A. Lowe and D. M. H. Sexton, 2014: Transient climate changes in a perturbed parameter ensemble of emissions-driven earth system model simulations. *Climate Dyn.,* **43,** 2855–2885, doi:10.1007/s00382-014-2097-5.

Nam, C., S. Bony, J.-L. Dufresne, and H. Chepfer, 2012: The 'too few, too bright' tropical low-cloud problem in CMIP5 models. *Geophys. Res. Lett.,* **39,** L21801.

Nguyen, H., A. Evans, C. Lucas, I. Smith, and B. Timbal, 2013: The Hadley circulation in reanalyses: Climatology, variability, and change. *J. Climate,* **26,** 3357–3376.

Nicholls, N., C. Landsea, and J. Gill, 1998: Recent trends in Australian region tropical cyclone activity. *Meteorol. Atmos. Phys.,* **65,** 197–205.

Nigam, S., Y. Zhao, A. Ruiz-Barradas and T. Zhou, 2015: The South-Flood North-Drought pattern over eastern China and the drying of the Gangetic Plain. Chao. 22 in Climate Change: Multidecadal and Beyond. Eds. C.P. Chang, M. Ghil, M. Latif, J. M. Wallace. World Scientific Series on Asia-Pacific Weather and Climate, Vol. 6, World Scientific, Singapore. 347-359. doi: 10.1142/9789814579933_0022.

842 Oh, H., K.-J. Ha, and A. Timmermann, 2018: Disentangling impacts of dynamic and thermodynamic
843 components on late summer rainfall anomailes in East Asia, *J. Geophys. Res.,* **123,** 8623–8633,
844 doi:10.1029/2018JD028652.
845 Omondi, P., L. A. Ogallo, R. Anya, J. M. Muthama, J.Ininda, 2013: Linkages between global sea surface
846 temperatures and decadal rainfall variability over Eastern Africa region. *Int. J. Climatol.,* **33,** 2082–
847 2104.
848 Panthou, G., T. Vischel, and T. Lebel, 2014: Recent trends in the regime of extreme rainfall in the Central
849 Sahel. *Int. J. Climatol.,* **3,** 3998–4006.
850 Pascale, S., W. R. Boos., S. Bordoni., T. L. Delworth, S. B. Kapnick, H. Murakami1, G. A. Vecchi, and W.
851 Zhang, 2017: Weakening of the North American monsoon with global warming. *Nat. Clim. Change,*
852 **7,** 806–812.
853 Pascale, S., L. M. Carvalho, D. K. Adams, C. L. Castro, and I. F. A. Cavalcanti, 2019: Current and future
854 variations of the monsoons of the Americas in a warming climate, *Curr. Clim. Change Rep.,* **5,** 125–
855 144.
856 Polson, D., M. Bollasina, G. C. Hegerl, and L. J. Wilcox, 2014: Decreased monsoon precipitation in the
857 Northern Hemisphere due to anthropogenic aerosols. *Geophys. Res. Lett.,* **41,** 6023–6029.
858 doi:10.1002/2014GL060811.
859 Prein, A. F., R. M. Rasmussen, K. Ikeda, C. Liu, M. P. Clark, and G. J. Holland, 2016: The future intensification
860 of hourly precipitation extremes. *Nature Climate Change,* **7,** 48–52.
861 Privé, N. C. and R. A. Plumb, 2007: Monsoon dynamics with interactive forcing. Part I: Axisymmetric studies.
862 *J. Atmos. Sci.,* **64,** 1417–1430.
863 Richardson, T. B., P. M. Forster, T. Andrews, O. Boucher, G. Faluvegid, D. Fläschner, Ø. Hodnebrog, M.
864 Kasoar, A. Kirkevåg, J.-F. Lamarque, G. Myhre, D. Olivié, B. H. Samset, D. Shawki, D. Shindell, T.

865 Takemura, and A. Voulgarakis, 2018: Drivers of precipitation change: An energetic understanding.
866 *J. Climate,* **31,** 9641–9657.
867 Rotstayn, L. D., W. Cai, M. R. Dix, G. D. Farquhar, Y. Feng, P. Ginoux, M. Herzog, A. Ito, J. E. Penner, M. L.
868 Roderick, M. and Wang, 2007: Have Australian rainfall and cloudiness increased due to the remote
869 effects of Asian anthropogenic aerosols? *J. Geophys. Res.,* **112,** D09202,
870 doi:10.1029/2006jd007712.
871 Roxy, M. K., K. Ritika, P. Terray, R. Murtugudde, K. Ashok, and B. N. Goswami, 2015: Drying of Indian
872 subcontinent by rapid Indian Ocean warming and a weakening land-sea thermal gradient. *Nature*
873 *Communications,* **6,** 7423, doi:10.1038/ncomms8423.
874 Roxy, M. K., Ghosh, S., Pathak, A., Athulya, R., Mujumdar, M., Murtugudde, R., ... & Rajeevan, M., 2017:
875 A threefold rise in widespread extreme rain events over central India. Nature communications,
876 8, 708.
877 Sabeerali, C., and R. Ajayamohan, 2017: On the shortening of Indian summer monsoon season in a
878 warming scenario. *Climate Dynamics***,** 1-16.
879 Salzmann, M., 2016: Global warming without global mean precipitation increase? *Sci. Adv.,* **2,** e1501572.
880 Salzmann, M., H. Weser, and R. Cherian, 2014: J. Geophys. Res. Atmos. 119, 11321-11337.
881 Salzmann, M., and R. Cherian, 2015: On the enhancement of the Indian summer monsoon drying by Pacific
882 multidecadal variability during the latter half of the twentieth century. J. Geophys. Res. Atmos.
883 120(18), 9103-9118.
884 Sanogo, S., A. H. Fink, J. A. Omotosho, A. Ba, R. Redl, and V. Ermert, 2015: Spatio-temporal characteristics
885 of the recent rainfall recovery in West Africa. *Int. J. Climatol.,* **35,** 4589–4605.
886 Sarr, M. A., M. Zoromé, O. Seidou, C. R. Bryant, and P. Gachon, 2013: Recent trends in selected extreme
887 precipitation indices in Senegal–A changepoint approach. *J. Hydrology,* **505,** 326–334.

888 Seth, A., S. A. Rauscher, M. Biasutti, A. Giannini, S. J. Carmargo and M. Rojas, 2013: CMIP5 projected
889 changes in the annual cycle of precipitation in monsoon regions. *J. Climate,* **26,** 7328–7351,
890 doi:10.1175/JCLI-D-12-00726.1.
891 Sharmila, S., S. Joseph, A. Sahai, S. Abhilash, and R. Chattopadhyay, 2015: Future projection of Indian
892 summer monsoon variability under climate change scenario: An assessment from CMIP5 climate
893 models. *Global and Planetary Change,* **124,** 62–78.
894 Shawki, D., Voulgarakis, A. , Chakraborty, A., Kasoar, M., and J. Srinivasan, 2018: The South Asian monsoon
895 response to remote aerosols: Global and regional mechanisms, *J. Geophys. Res*., *Atmospheres,*
896 123, 11, 585–11,601.
897 Shi., H., B. Wang, Cook, E. D., J. Liu, and F. Liu, 2018: Asian Summer Precipitation over the Past 544 Years
898 Reconstructed by Merging Tree Rings and Historical Documentary Records**.** *J. Climate*, 31, 7845-
899 7861. DOI: 10.1175/JCLI-D-18-0003.1.
900 Shonk, J. P., A. G. Turner, A. Chevuturi, L. Wilcox, A. J. Dittus, and E. Hawkins, 2019: Uncertainty in aerosol
901 radiative forcing impacts the simulated global monsoon in the 20th century. *Geophys. Res. Letts.,*
902 revised version submitted. The latest version of this paper can be accessed at
903 https://livereadingac-my.sharepoint.com/:f:/g/personal/a_g_turner_reading_ac_uk/
904 El8hjGgHjs5KooEbLEP0lIIBGgSajLIwumjN9ARCV7lJNQ?e=GrH4NI.
905 Singh, M. S., Z. Kuang, and Y. Tian, 2017: Eddy inuences on the strength of the Hadley circulation: Dynamic
906 and thermodynamic perspectives. *J. Atmos. Sci.,* **74,** 467–486.
907 Singh, D., S. Ghosh, M. K. Roxy, and S. McDermid, 2019: Indian summer monsoon: Extreme events,
908 historical changes, and role of anthropogenic forcings. *WIREs Clim. Change*, e571,
909 doi:10.1002/wcc571.
910 Sigmond, M., and J. C. Fyfe, 2016: Tropical Pacific impacts on cooling North American winters. *Nature*
911 *Climate Change,* **6,** 970–974.

912 Skansi, M. M., M. Brunet, J. Sigró, E. Aguilar, J. A. A. Groening, O. J. Bentancur, Y. R. C. Geier, R. L. C. Amaya,
913 H. Jácome, A. M. Ramos, C. O. Rojas, A. M. Pasten, S. S. Mitro, C. V. Jiménez, R. Martínez, L. V.
914 Alexander, P.D. Jones, 2013: Warming and wetting signals emerging from analysis of changes in
915 climate extreme indices over South America. *Global and Planetary Change*, 100, 295-307.
916 doi:10.1016/j.gloplacha.2012.11.004.
917 Sobel, A. H., and J. D. Neelin, 2006: The boundary layer contribution to intertropical convergence zones in
918 the quasi-equilibrium tropical circulation model framework. *Theor. Comput. Fluid Dyn.,* **20,** 323–
919 350.
920 Sontakke NA, Singh N, Singh HN (2008) Instrumental period rainfall series of the Indian region (AD 1813-
921 2005): Revised reconstruction, update and analysis. Holocene 18:1055–1066.
922 https://doi.org/10.1177/0959683608095576
923 Sooraj, K., P. Terray, and P. Xavier, 2016: Sub-seasonal behaviour of Asian summer monsoon under a
924 changing climate: Assessments using CMIP5 models. *Climate Dyn.*, **46,** 4003–4025.
925 Sperber, K. R., H. Annamalai, I.-S. Kang, A. Kitoh, A. Moise, A. Turner, B. Wang, and T. Zhou, 2013: The
926 Asian summer monsoon: an intercomparison of CMIP5 vs. CMIP3 siulations of the late 20th
927 century. CLim. Dyn., 41, 2711-2744.
928 Taylor, C. M., D. Belušic, F. Guichard, D. J. Parker, T. Vischel, O. Bock, P. P. Harris, S. Janicot, C. Klein, and
929 Panthou, G., 2017: Frequency of extreme Sahelian storms tripled since 1982 in satellite
930 observations. *Nature,* **544,** 475–478.
931 Taylor, C. M., A. H. Fink, C. Klein, D. J. Parker, F. Guichard, P. P. Harris, and K.R. Knapp, 2018: Earlier
932 seasonal onset of intense mesoscale convective systems in the Congo Basin since 1999. *Geophys.*
933 *Res. Lett.,* **45,** 13458–13467, doi:10.1029/2018GL080516.
934 Timbal, B. and W. Drosdowsky, 2013: The relationship between the decline of South Eastern Australia
935 rainfall and the strengthening of the sub-tropical ridge. *Int. J. Clim.,* **33,** 1021–1034.

936 Turner, A. G., G. S. Bhat et al., 2019: Interaction of Convective Organisation with Monsoon Precipitation,
937 Atmosphere, Surface and Sea: the 2016 INCOMPASS field campaign in India. *Quarterly Journal of*
938 *the Royal Meteorological Society*, doi: 10.1002/qj.3633.
939 Vera, C. S., and L. Diaz, 2015: Anthropogenic influence on summer precipitation trends over South America
940 in CMIP5 models. *Int. J. Climatol.*, **35,** 3172–3177, doi:10.1002/joc.4153.
941 Wang, B., and Q. Ding, 2006: Changes in global monsoon precipitation over the past 56 years. Geophys.
942 Res. Lett., 33, L06711, doi: 10.1029/2005GL025347.
943 Wang, B., and Q. Ding, 2008: Global monsoon: Dominant mode of annual variation in the
944 tropics. *Dynamics of Atmos. and Ocean, special issue 2,* doi: 10.1016/j.dynatmoce.2007.05.002.
945 Wang, B., C. Jin, and J. Liu, 2019: Future change of global monsoon projected by CMIP6 models. *J Climate*,
946 Revised version submitted.
947 Wang, B., Liu J, Kim HJ, Webster PJ, and Yim SY, 2012: Recent Change of the Global Monsoon Precipitation
948 (1979-2008). *Climate Dyn.*.,39, 1123-1135, doi: 10.1007/s00382-011-1266-z.
949 Wang, B., J. Liu, H.-J. Kim, P. J. Webster, S.-Y. Yim, and B. Xiang, 2013: Northern Hemisphere summer
950 monsoon intensified by mega-El Nino/southern oscillation and Atlantic multidecadal oscillation.
951 *Proc. Nat. Acad. Sci.,* **110,** 5347–5352.
952 Wang, B., S-Y. Yim, J.-Y. Lee, J. Liu, and K.-J. Ha, 2014: Future change of Asian-Australian monsoon under
953 RCP 4.5 anthropogenic warming scenario. *Climate Dyn.,* **42,** 83–100.
954 Wang, B., J. Li, M.A. Cane, J. Liu, P.J. Webster, B. Xiang, H.-M. Kim, J. Cao, and K.-J. Ha, 2018: Toward
955 predicting changes in land monsoon rainfall a decade in advance. *J. Climate,* **31,** 2699–2714.
956 Wang, P.-X., B. Wang, H. Cheng, J. Fasullo, Z. T. Guo, T. Kiefer, Z. Y. Liu, 2014: The Global Monsoon across
957 Time Scales: Is there coherent variability of regional monsoons? Climate of the Past., 10, 2163-
958 2291.

Wang, P.-X., B. Wang, H. Cheng, J. Fasullo, Z. Guo, T. Kiefer, and Z. Liu, 2017: The Global Monsoon across Time Scales: Mechanisms and Outstanding Issues. Earth Science Reviews, 174, 82-121.

Willetts, P. D., J. H. Marsham, C. E. Birch, D. J. Parker, S. Webster, and J. Petch, 2017: Moist convection and its upscale effects in simulations of the Indian monsoon with explicit and parametrized convection. *Q. J. R. Meteorol. Soc.,* 143, 1073-1085, doi:10.1002/qj.2991.

Wright, J. S., R. Fu, J. R. Worden, S. Chakraborty, N. E. Clinton, C. Risi, Y. Sun and L. Yin, 2017: Rainforest-initiated wet season onset over the southern Amazon. *Proceedings of the National Academy of Sciences*, 114(32).

Wu, M., Y. Luo, F. Chen, and W. K. Wong, 2019: Observed link of extreme hourly precipitation changes to urbanization over coastal South China. J. Appl. Meteor. Climatol., 58, 1799-1819, doi:10.1175/JAMC-D-18-0284.1.

Yang, Y., L. M. Russell, S. Lou, H. Liao, J. Guo, Y. Liu, B. Singh, and S. J. Ghan, 2017: Dust-wind interactions can intensify aerosol pollution over eastern China. *Nature Communications,* **8,** 15333, doi:10.1038/ncomms15333.

Yin, L., R. Fu, E. Shevliakova, and R. E. Dickinson, 2013: How well can CMIP5 simulate precipitation and its controlling processes over tropical South America? *Climate Dyn.,* **41,** 3127–3143, doi:10.1007/s00382-012-1582-y.

Ying, J., P. Huang, T. Lian, and H. Tan, 2019: Understanding the effect of an excessive cold tongue bias on projecting the tropical Pacific SST warming pattern in CMIP5 models. *Climate Dyn.,* **52,** 1805–1818.

Yuan, X., S. Wang, and Z.-Z. Hu 2018: Do climate change and El Niño increase likelihood of Yangtze River extreme rainfall? [in “Explaining Extreme Events of 2016 from a Climate Perspective”]. Bull. Amer. Meteor. Soc., 99 (1), S113-S117. doi: 10.1175/BAMS-D-17-0089.1.

Zelinka,M. D., T. A. Myers, D. T. McCoy, S. Po-Chedley, P. M. Caldwell , P. Ceppi, S. A. Klein , and K. E. Taylor, 2020: Causes of higher climate sensitivity in CMIP6 models. Geophysical Research Letter, 47, e2019GL085782.

Zhang, W., T. Zhou, L. Zhang, and L. Zou, 2019: Future intensification of the water cycle with an enhanced annual cycle over global land monsoon regions. *J. Climate*, **32,** 5437–5452.

Zhang, W., T. Zhou, L. Zou, L. Zhang, and X. Chen, 2018: Reduced exposure to extreme precipitation from 0.5°C less warming in global land monsoon regions. Nat. Commun., https://doi.org/10.1038/s41467-018-05633-3.

Zhang, W., Zhou, T. 2019: Significant increases in extreme precipitation and the associations with global warming over the global land monsoon regions. Journal of Climate, https://doi.org/10.1175/JCLI-D-18-0662.1.

Zheng, F., J. P. Li, and T. Liu, 2014: Some advances in studies of the climatic impacts of the Southern Hemisphere annular mode. J. Meteor. Res., 28, 820-835.

Zhou, T., D. Gong, J. Li, and B. Li, 2009: Detecting and understanding the multi-decadal variability of the East Asian Summer Monsoon – Recent progress and state of affairs. *Meteorologische Zeitschrift,* **18,** 455–467.

Zhou, L. M., Y. H. Tian, R. B. Myneni, P. Ciais, S. Saatchi, Y. Y. Liu, S. L. Piao, H. S. Chan, E. F. Vermote, and co-authors, 2014: Widespead decline of Congo rainforest greenness in the past decade. *Nature,* **509,** 86–89, doi:10.1038/nature13265.

Zhou, T., J. Lu and W. Zhang, 2020a: The sources of uncertainty in the projection of global land monsoon precipitation. *Geophys. Res. Lett.,* under review. Pdf file available at: https://drive.google.com/open?id=1hkuL4G_xQ-2B6PBYGSMHXDhBrcAARaPZ

.

1004 Zhou T., W. Zhang, L. Zhang, X. Zhang, Y. Qian, D. Peng, S. Ma, B. Dong, 2020b: The dynamic and
1005 thermodynamic processes dominating the reduction of global land monsoon precipitation driven
1006 by anthropogenic aerosols emission. *Science China: Earth Sciences*, accepted and in press.
1007 Zhu, C. W., B. Wang, W. H. Qian, and B. Zhang, 2012: Recent Weakening of Northern East Asian Summer
1008 Monsoon: A Possible Response to Global Warming. *Geophys. Res. Lett.,* **39,** L09701, doi:
1009 10.1029/2012GL051155.
1010

Figure captions

Figure 1. The GM precipitation domain (in Green) defined by the local summer-minus-winter precipitation rate exceeds 2 mm day^{-1}, and the local summer precipitation exceeds 55 % of the annual total (Wang and Ding 2008). Summer denotes May through September for the North ern Hemisphere and November through March for the Southern Hemisphere. The dry regions (in yellow) is defined by local summer precipitation being less than 1 mm day^{-1}. The arrows show August-minus-February 925 hPa winds. The blue (red) lines indicate the ITCZ position in August (February). Adopted from P.X. Wang et al. (2014).

Figure 2: Past to future changes of annual-mean global monsoon precipitation (mm/day) over (a) land and (b) ocean relative to the recent past (1995-2014) in historical simulation (1850-2014) and four core SSPs (2015-2100) obtained from 34 CMIP6 models. Pink and mid-blue shading indicate 5%-95% likely range of precipitation change in low emission (SSP1-2.6) and high emission (SSP5-8.5) scenario, respectively. The mean change during 2081-2100 relative to the recent past is also shown with the box plot in right-hand side obtained from four SSPs in 34 CMIP6 models compared to RCP 8.5 in 40 CMIP5 models. The solid dot in the box plot for SSP5-8.5 indicates individual model's equilibrium climate sensitivity (ECS).

Fig. 3 Projected regional land monsoon precipitation sensitivity under the SSP2-4.5, i. e., the percentage change (2065–2099 relative to 1979–2013) per 1^{o}C global warming, in units of %/^{o}C) derived from 24 CMIP6 models for (a) local summer, (b) local winter, and (c) annual mean land monsoon precipitation for each region. Local summer means JJAS in NH and DJFM for SH, and local winter means the opposite. The upper edge of the box represents the 83th percentile and the lower edge is the 17th percentile, so the box contains 66% of the model

1033 projection data and represents the “likely” range. The horizontal line within the box is the
1034 median. Red circle is the mean. The vertical dash line segments represent the “very likely”
1035 range from 5% to 95%.
1036 **Fig. 4** Changes in the annual mean (a) precipitation, (b) 850 hPa specific humidity, and (c)
1037 surface air temperature. Changes are measured by the SSP2-4.5 projection (2065–2099)
1038 relative to the historical simulation (1979–2013) in the 24 models’ MME. The color shaded
1039 region denotes the changes are statistically significant at 66% confidence level (likely change).
1040 Stippling denotes areas where the significance exceeds 95% confidence level (very likely) by
1041 student t-test.
1042 **Fig. 5** Schematic main features related to present (left panel) and future (right panel) changes
1043 for the North American Monsoon (left). The expansion and northwestward shift of the NAM
1044 ridge, the southward shift of the upper-level inverted troughs (IVs) track, and the strengthening
1045 of the remote stabilizing effect due to SST warming are shown. Red and blue shading indicates
1046 drying and wettening, respectively, due to the large- scale shifts. Larger clouds in the lower
1047 panel is suggestive of more intense MCS-type convection. A question mark (?) on the lower
1048 panels indicates uncertainty in the response, as it is the case, for example, for the local
1049 mechanisms associated with atmosphere-land interaction, NAM moisture surges and
1050 southward shift the tropical easterly waves (TEWs) track.
1051 **Figure 6**. Time series of extreme precipitation events observed at Seoul, Korea since 1778.
1052 Running five-year means of the summer highest one-day precipitation amount (green, mm/day
1053 in the left y-axis), the number of extremely wet days (blue, right y-axis) and the precipitation
1054 amount falling in the extremely wet days (red, mm/day in the left axis). The extremely wet days

1055 are calculated as the 99th percentile of the distribution of the summer daily precipitation
1056 amount in the 227-year period. Also shown are the corresponding trends obtained by least-
1057 square regression for the green curve and logistic regression for the blue and red curve.
1058 Adopted from Wang et al. (2006)
1059 **Figure 7**. Frequency of extreme rain events (number of grid cells exceeding 150 mm/day per
1060 year) over central Indian subcontinent (75°–85° E, 19°–26° N) for the summer monsoon (June-
1061 September) during 1950–2015. The trend lines shown in the figures are significant at 95%
1062 confidence level. The smoothed curves on the time series analyses represent 10-year moving
1063 averages. Adopted from Roxy et al. (2017).
1064 **Figure 8** The surface air temperature and extremely hourly rainfall trends for urban stations and
1065 rural stations in the Yangzi River Delta, calculated from changes from 1975-1996 to 1975-2018,
1066 during MJJAS. (From Jiang et al. 2020); CP: please check this caption. Is "1975-2018 correct? In the
1067 caption should we explain the meaning of the thick cross (red and blue)?
1068 **Figure 9** (a) RCP8.5 (2050-2100) minus HIST (1950-2000) differences in band-pass-filtered daily
1069 rainfall standard deviation (%) for Australian (red, left boxes), South Asian (purple, center
1070 boxes) and East Asian (green, right boxes) monsoon domain. Data are DJFM months for AUS
1071 and JJAS months for SA and EA. Daily data are band-pass-filtered for the set of bands indicated
1072 on the x-axis. (c) and (d) are the multi-model mean change in standard deviation of *daily* rainfall
1073 (%) from HIST (1950-2000) to RCP8.5 (2050-2100) in (c) DJFM and (d) JJAS. The South Asian (SA),
1074 East Asian (EA) and Australian (AUS) monsoon domains are shown in the relevant wet season.
1075 (from Brown et al. 2017).
1076

Supplementary Figures

Figure S1 The response of Northern African precipitation to CO2 increase as simulated by CMIP6 models. (left) Annual mean differences in rainfall between years 81-100 and 1-20 of the 1pctCO2 simulation, expressed as percentage of the 1-20 mean, averaged across 13 models. (right) The monthly climatology of the rainfall difference across the same periods for individual models (grey) and the multi-model mean (black) for (top) West Sahel (18W-10W, 10N-20N) and (bottom) East Sahel (10W-35E, 10N-20N). The models used are: CAMS-CSM1-0, GFDL-CM4, MRI-ESM2-0, GFDL-ESM4, MIROC6, CNRM-CM6-1, BCC-ESM1, CNRM-ESM2-1, CanESM5, IPSL-CM6A-LR, BCC-CSM2-MR, HadGEM3-GC31-LL, UKESM1-0-LL.

Figure S2 Daily climatological precipitation (mm day^{-1}) averaged over 35° E - 42° E and 3° S - 3° N for the CHIRPS V2.0 1995 – 2014 climatology (black lines), the last 20 years of the CMIP6 historical experiment (red lines;1995-2014), and the last 20 years of the CMIP6 SSP2 4.5 experiment (blue lines; 2081-2100) for various individual CMIP6 CGCM and ESM models (a – g). (h) shows the multi-model mean of the 7 CMIP6 models.

Figure S3 Daily climatological precipitation (mm day-1) averaged over 10° E - 30° E and 5° S - 5° N for the CHIRPS V2.0 1995 – 2014 climatology (black lines), the last 20 years of the CMIP6 historical experiment (red lines; 1995-2014), and the last 20 years of the CMIP6 SSP2 4.5 experiment (blue lines; 2081-2100) for various individual CMIP6 CGCM and ESM models (a – g). (h) shows the multi-model mean of the 7 CMIP6 models.

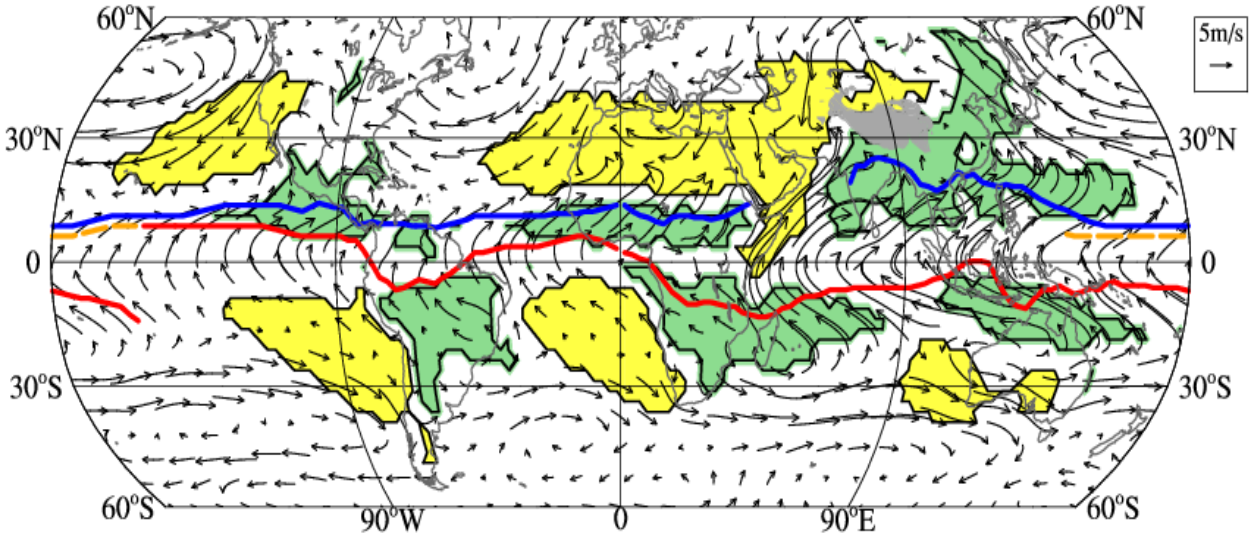

Figure 1. The GM precipitation domain (in Green) defined by the local summer-minus-winter precipitation rate exceeds 2 mm day^{-1}, and the local summer precipitation exceeds 55 % of the annual total (Wang and Ding 2008). Summer denotes May through September for the Northern Hemisphere and November through March for the Southern Hemisphere. The dry regions (in yellow) is defined by local summer precipitation being less than 1 mm day^{-1}. The arrows show August-minus-February 925 hPa winds. The blue (red) lines indicate the ITCZ position in August (February). Adopted from P.X. Wang et al. (2014).

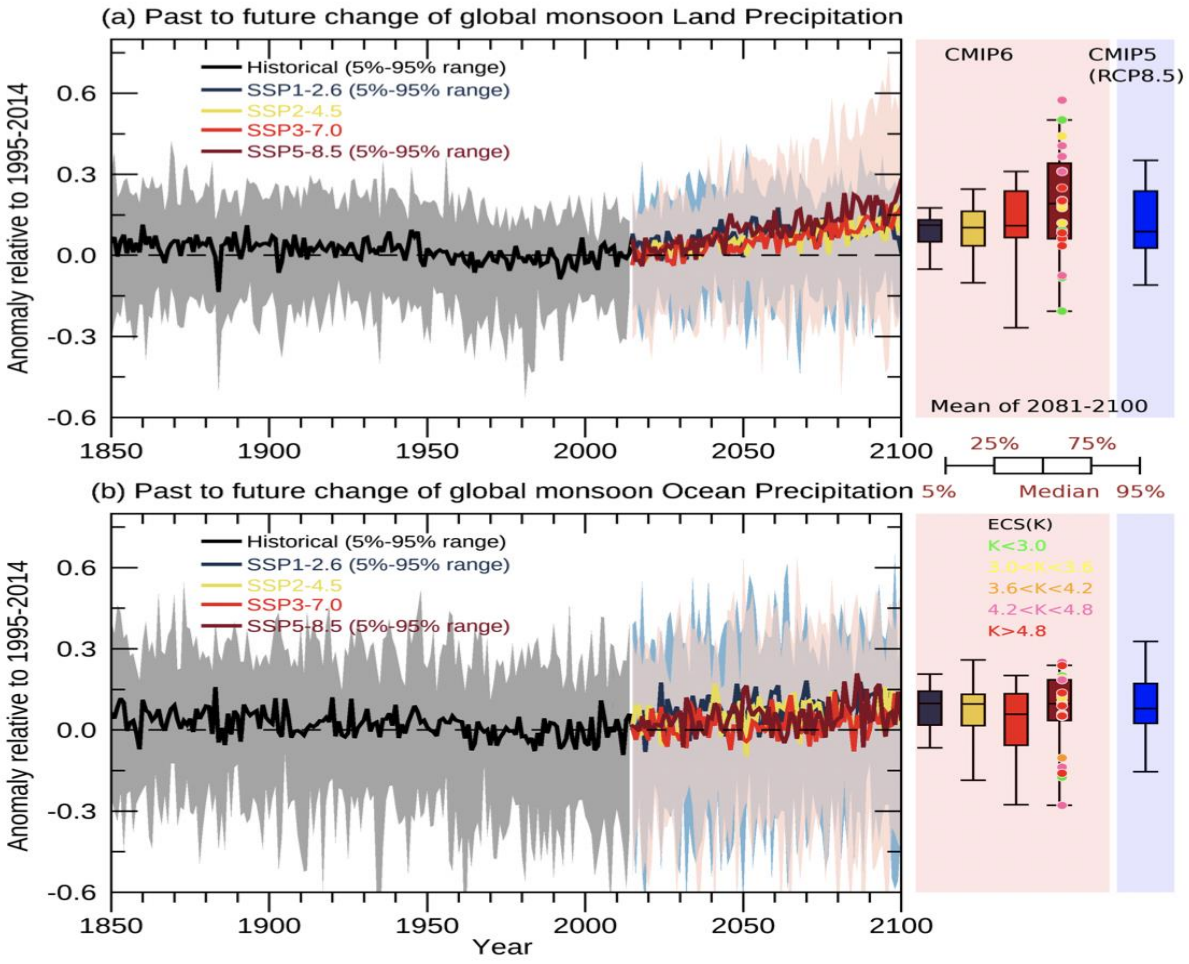

Fig. 2 Past to future changes of annual-mean global monsoon precipitation (mm/day) over (a) land and (b) ocean relative to the recent past (1995-2014) in historical simulation (1850-2014) and four core SSPs (2015-2100) obtained from 34 CMIP6 models. Pink and mid-blue shading indicate 5%-95% likely range of precipitation change in low emission (SSP1-2.6) and high emission (SSP5-8.5) scenario, respectively. The mean change during 2081-2100 relative to the recent past is also shown with the box plot in right-hand side obtained from four SSPs in 34 CMIP6 models compared to RCP 8.5 in 40 CMIP5 models. The solid dot in the box plot for SSP5-8.5 indicates individual model's equilibrium climate sensitivity (ECS).

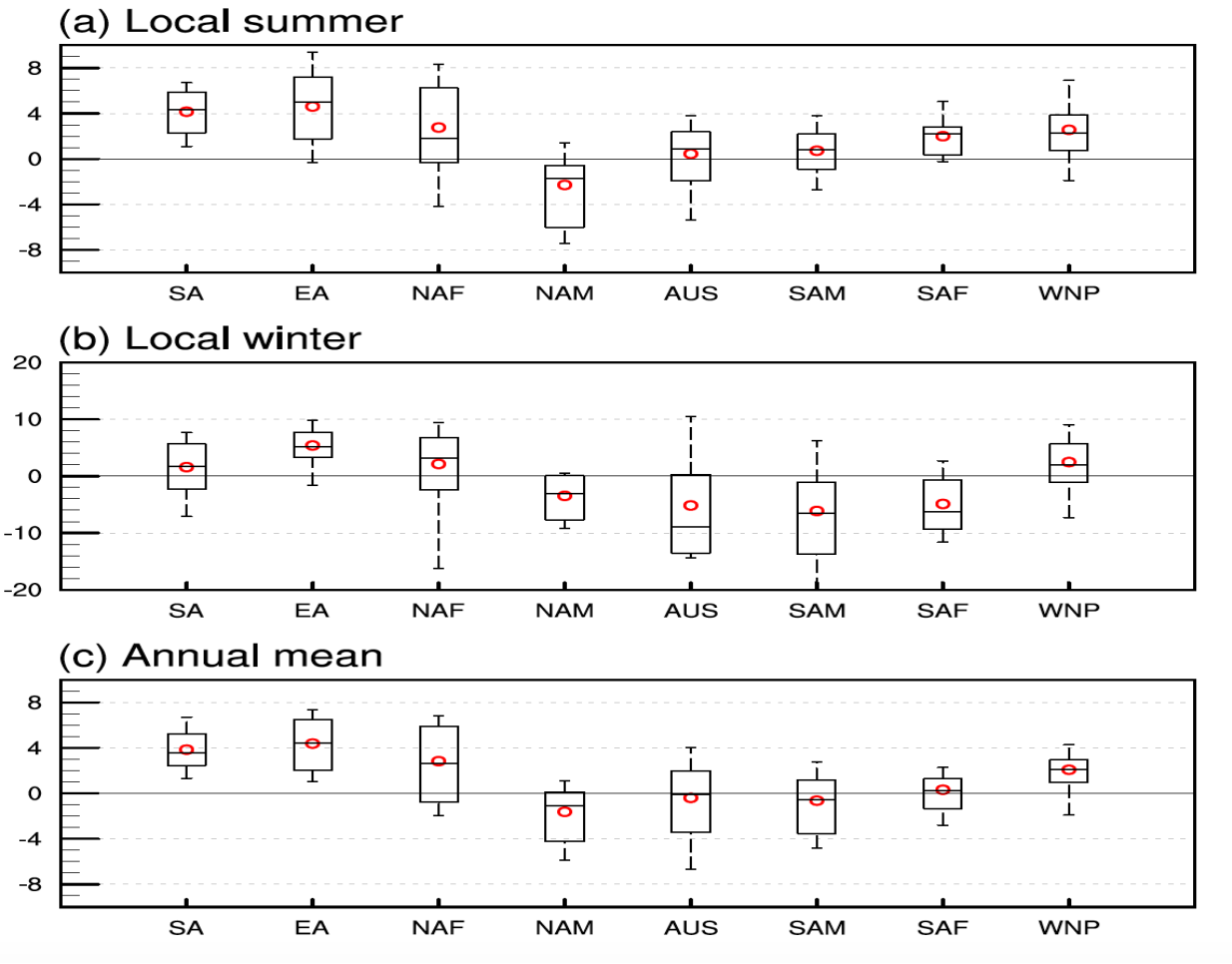

Fig. 3 Projected regional land monsoon precipitation sensitivity under the SSP2-4.5, i. e., the percentage change (2065–2099 relative to 1979–2013) per 1°C global warming, in units of %/°C) derived from 24 CMIP6 models for (a) local summer, (b) local winter, and (c) annual mean land monsoon precipitation for each region. Local summer means JJAS in NH and DJFM for SH, and local winter means the opposite. The upper edge of the box represents the 83th percentile and the lower edge is the 17th percentile, so the box contains 66% of the model projection data and represents the "likely" range. The horizontal line within the box is the median. Red circle is the mean. The vertical dash line segments represent the "very likely" range from 5% to 95%.

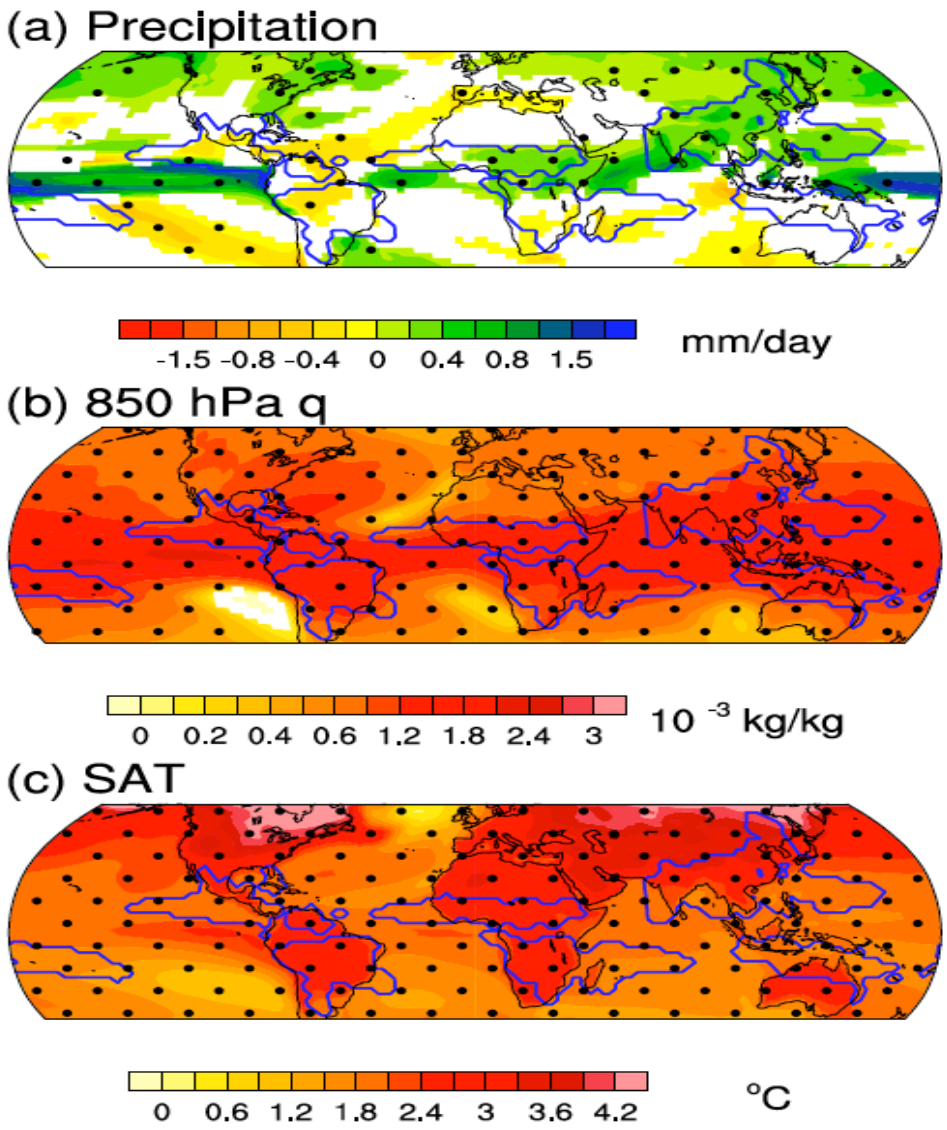

1127

1128 Fig. 4 Changes in the annual mean (a) precipitation, (b) 850 hPa specific humidity, and (c)
1129 surface air temperature. Changes are measured by the SSP2-4.5 projection (2065–2099)
1130 relative to the historical simulation (1979–2013) in the 15 models' MME. The color shaded
1131 region denotes the changes are statistically significant at 66% confidence level (likely change).
1132 Stippling denotes areas where the significance exceeds 95% confidence level (very likely) by
1133 student t-test.

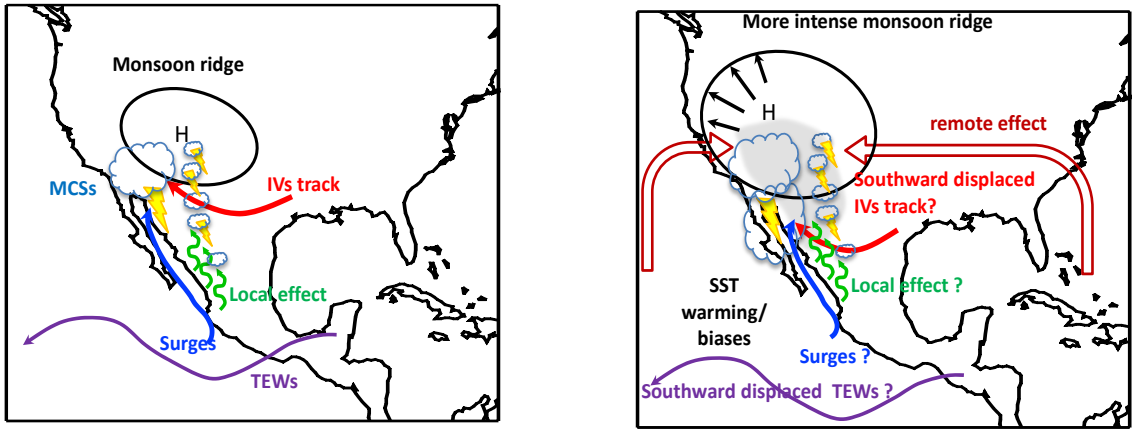

1134

1135 Fig. 5: Schematic main features related to present (left panel) and future (right panel) changes
1136 for the North American Monsoon (left). The expansion and northwestward shift of the NAM
1137 ridge, the southward shift of the upper-level inverted troughs (IVs) track, and the strengthening
1138 of the remote stabilizing effect due to SST warming are shown. Red and blue shading indicates
1139 drying and wettening respectively due to the large- scale shifts. Larger clouds in the lower panel
1140 is suggestive of more intense MCS-type convection. A question mark (?) on the lower panels
1141 indicates uncertainty in the response, as it is the case, for example, for the local mechanisms
1142 associated with atmosphere-land interaction, NAM moisture surges and southward shift the
1143 tropical easterly waves (TEWs) track.

1144

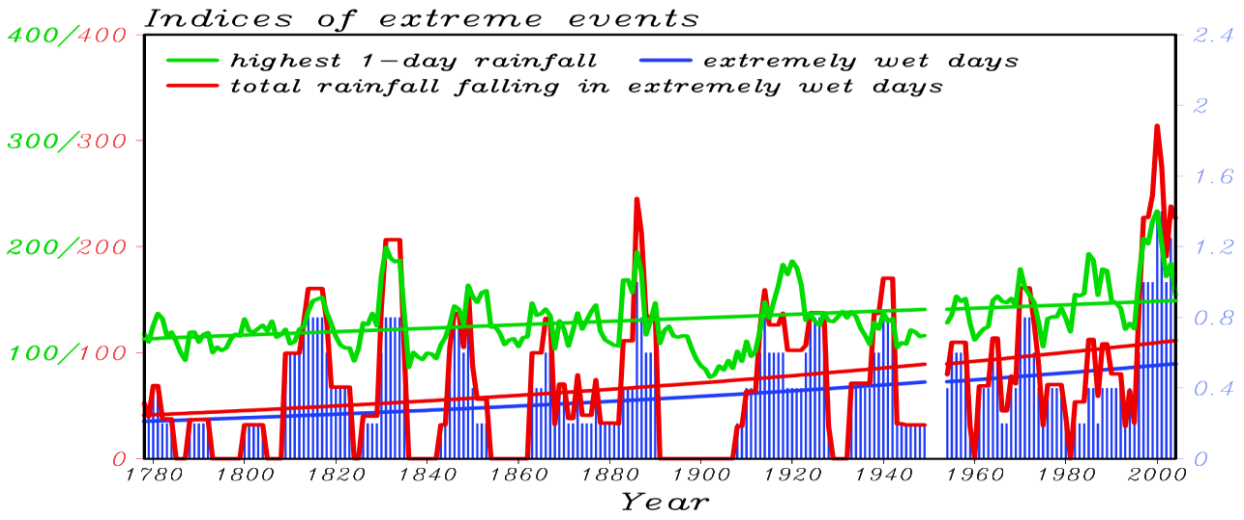

1145

1146 Figure 6. Time series of extreme precipitation events observed at Seoul, Korea since 1778.
1147 Running five-year means of the summer highest one-day precipitation amount (green, mm/day
1148 in the left y-axis), the number of extremely wet days (blue, right y-axis) and the precipitation
1149 amount falling in the extremely wet days (red, mm/day in the left axis). The extremely wet days
1150 are calculated as the 99th percentile of the distribution of the summer daily precipitation
1151 amount in the 227-year period. Also shown are the corresponding trends obtained by least-
1152 square regression for the green curve and logistic regression for the blue and red curve.
1153 Adopted from Wang et al. (2006)

1154

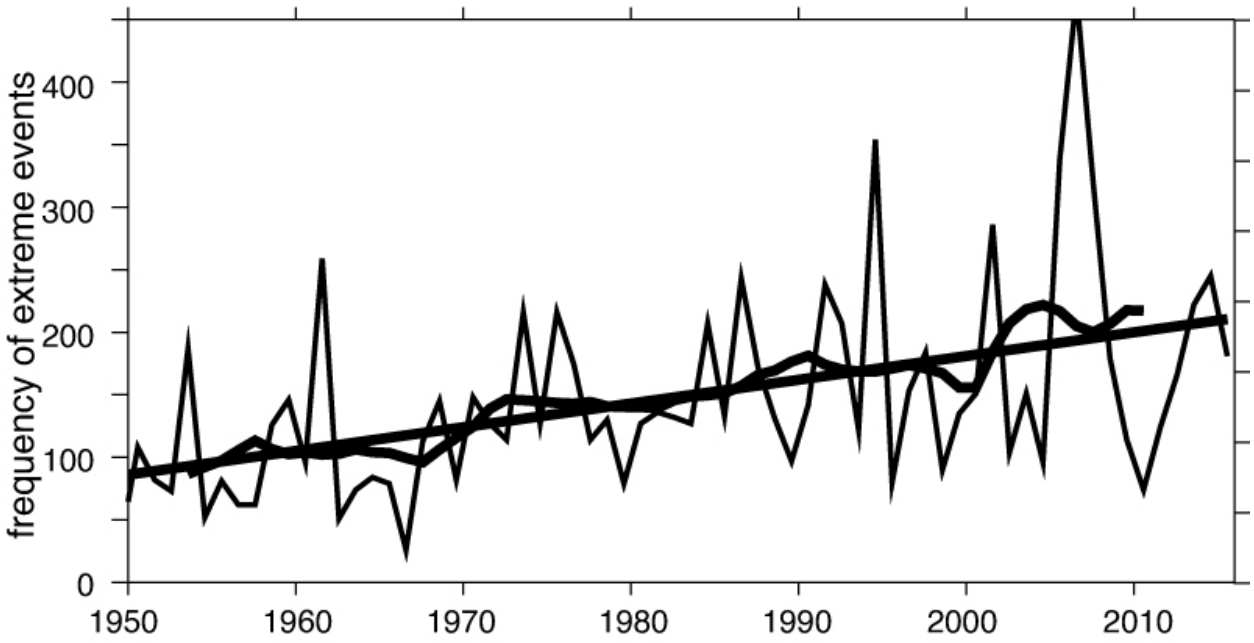

Figure 7. Frequency of extreme rain events (number of grid cells exceeding 150 mm/day per year) over central Indian subcontinent (75°–85° E, 19°–26° N) for the summer monsoon (June-September) during 1950–2015. The trend lines shown in the figures are significant at 95% confidence level. The smoothed curves on the time series analyses represent 10-year moving averages. Adopted from Roxy et al. (2017).

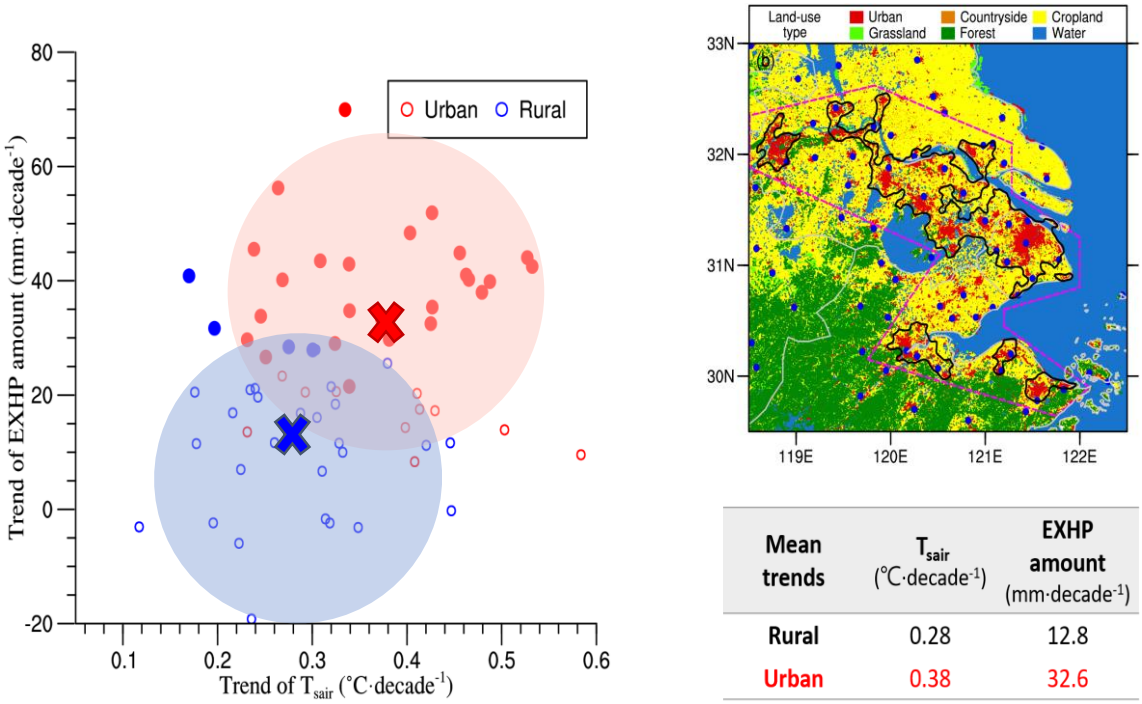

Mean trends	T_{sair} (°C·decade^{-1})	EXHP amount (mm·decade^{-1})
Rural	0.28	12.8
Urban	0.38	32.6

Figure 8 The surface air temperature and extremely hourly rainfall trends (EXHP) for urban stations and rural stations in the Yangzi River Delta, calculated from changes from 1975-1996 to 1975-2018, during MJJAS. (From Jiang et al. 2020).

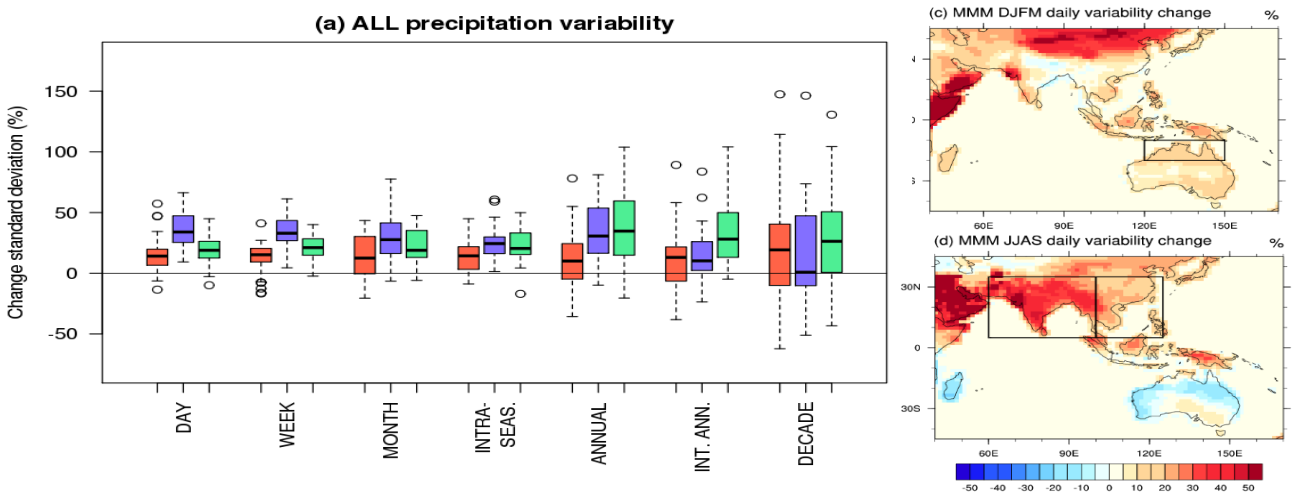

Fig. 9 (a) RCP8.5 (2050-2100) minus HIST (1950-2000) differences in band-pass-filtered daily rainfall standard deviation (%) for Australian (red, left boxes), South Asian (purple, center boxes) and East Asian (green, right boxes) monsoon domain. Data are DJFM months for AUS and JJAS months for SA and EA. Daily data are band-pass-filtered for the set of bands indicated on the x-axis. (c) and (d) are the multi-model mean change in standard deviation of *daily* rainfall (%) from HIST (1950-2000) to RCP8.5 (2050-2100) in (c) DJFM and (d) JJAS. The South Asian (SA), East Asian (EA) and Australian (AUS) monsoon domains are shown in the relevant wet season. (from Brown et al. 2017).